

Zeitschrift: IABSE reports = Rapports AIPC = IVBH Berichte
Band: 57/1/57/2 (1989)
Rubrik: Poster Session 3

Nutzungsbedingungen

Die ETH-Bibliothek ist die Anbieterin der digitalisierten Zeitschriften auf E-Periodica. Sie besitzt keine Urheberrechte an den Zeitschriften und ist nicht verantwortlich für deren Inhalte. Die Rechte liegen in der Regel bei den Herausgebern beziehungsweise den externen Rechteinhabern. Das Veröffentlichen von Bildern in Print- und Online-Publikationen sowie auf Social Media-Kanälen oder Webseiten ist nur mit vorheriger Genehmigung der Rechteinhaber erlaubt. [Mehr erfahren](#)

Conditions d'utilisation

L'ETH Library est le fournisseur des revues numérisées. Elle ne détient aucun droit d'auteur sur les revues et n'est pas responsable de leur contenu. En règle générale, les droits sont détenus par les éditeurs ou les détenteurs de droits externes. La reproduction d'images dans des publications imprimées ou en ligne ainsi que sur des canaux de médias sociaux ou des sites web n'est autorisée qu'avec l'accord préalable des détenteurs des droits. [En savoir plus](#)

Terms of use

The ETH Library is the provider of the digitised journals. It does not own any copyrights to the journals and is not responsible for their content. The rights usually lie with the publishers or the external rights holders. Publishing images in print and online publications, as well as on social media channels or websites, is only permitted with the prior consent of the rights holders. [Find out more](#)

Download PDF: 09.07.2025

ETH-Bibliothek Zürich, E-Periodica, <https://www.e-periodica.ch>



POSTER

Leere Seite
Blank page
Page vide

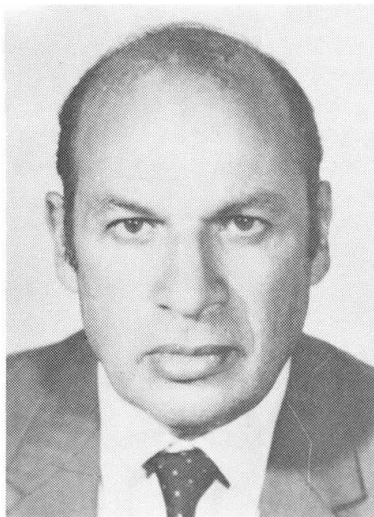
Behaviour and Analysis of Voided Concrete Slabs

Comportement et analyse des dalles creuses en béton

Verhalten und Analyse von Beton-Hohlplatten

S. A. EL-BEHAIRY

Professor
Ain Shams Univ.
Cairo, Egypt



S. A. El-Behairy, born in 1936, received his B. Sc. degree in civil eng. at Cairo Univ. in 1959, his Ph. D. from Karlsruhe Univ., FR Germany in 1965. Spend 8 years teaching at El Riad Univ. in Saudi Arabia. Now he is professor at Ain Shams Univ. in Cairo, Egypt.

M. I. SOLIMAN

Assist. Professor
Ain Shams Univ.
Cairo, Egypt



M. I. Soliman, born in 1946, received his B. Sc. degree in civil eng. from Ain Shams Univ., Cairo in 1969, his M. Sc. deg. from the same Univ. in 1972. He got a M. Eng. deg. from McGill Univ., Canada in 1975 and his Ph. D. in 1979 from the same university.

N. A. FOUAD

Research Assist.
Ain Shams Univ.
Cairo, Egypt



N. A. Fouad, born in 1964, received his B. Sc. degree in civil eng. from Ain Shams Univ., Cairo in 1986. He is a research assist. at the mentioned univ. and for the time being he is preparing for his M. Sc. degree.

SUMMARY

An experimental-theoretical study was conducted to explain the general deformational behaviour of voided reinforced concrete slabs under different loading conditions. Six voided reinforced concrete slabs were tested. The varying parameters were the void's diameter and the percentage of reinforcement. The experimental results are compared with those obtained theoretically using the orthotropic plate theories. The effect of crack on the slabs behaviour was studied. General conclusions are summarized.

RÉSUMÉ

Une étude expérimentale et théorique a été conduite pour définir le comportement général de déformation des dalles creuses en béton armé sous différents cas de charge. Six dalles ont été testées. Les paramètres variables étaient le diamètre du creux et le pourcentage de renforcement. Des conclusions générales sont présentées.

ZUSAMMENFASSUNG

Eine experimentelle und theoretische Studie wurde durchgeführt, um die allgemeine Verhaltensweise von Stahlbeton-Hohlplatten unter verschiedener Belastung zu ermitteln. Sechs Stahlbeton-Hohlplatten mit verschiedenen kreisförmigen Aussparungen oder unterschiedlicher Bewehrung wurden getestet. Die Ergebnisse der Versuche wurden mit denen der Theorie orthotropen Platten verglichen. Die Wirkung von Rissen auf das Verhalten der Hohlplatten wurde studiert. Allgemeine Schlussfolgerungen werden dargelegt.



1. INTRODUCTION

Circular voids running in the longitudinal direction of reinforced concrete slabs are frequently introduced in order to reduce the self weight of the structure. This type of slabs are used in the construction of floor slabs, short and medium span slab bridges. Voids of circular shape are simpler for construction. Furthermore, the stress concentration around these voids is less critical than any other shape.

The presented study is concerned with the general deformational behaviour of the reinforced concrete voided slabs under symmetrical and unsymmetrical cases of loading. Six voided reinforced concrete slabs of dimensions 1.04x1.8 m, having void diameters of 63, 50 and 40 mm, and different reinforcement percentages, were tested.

The cross distribution of deflections, longitudinal moments and transverse moments were calculated using the orthotropic plate theory, and these results were compared with those obtained experimentally. The effect of longitudinal and transverse cracking on the behaviour of the slabs is studied. From the results of this experimental-theoretical study, conclusions are drawn concerning the design, construction and the evaluation of the stiffnesses of this type of structures.

2. METHOD OF ANALYSIS OF VOIDED SLABS

Simply supported right voided slabs subject to different concentrated loads, are generally analysed using the orthotropic plate theory. This load distribution theory was first introduced by Guyon (1946) & Massonnet (1950), which was formulated into a design procedure by Morice and Little (1956) and Rowe (1962). Morice, Little and Rowe also presented this method in the form of design charts (1956).

The theory assumes that the voided slab or bridge, being analysed, can be simulated as an equivalent orthotropic plate having the same average stiffness properties as the actual bridge or slab. This assumption is valid if there is no significant cell distortion.

Cusens and Pama (1969) prepared new design charts, by which the 10 % under-estimation in the early load distribution theory by Morice, Little and Rowe is being avoided.

To consider the effect of cell distortion in the analysis, Massonnet and Gandolfi (1967), developed a theory for shear weak rectangular orthotropic plates, which are simply supported on two opposite sides. Furthermore, Bakht, Jagear & Cheung (1981) simplified the previous method by introducing the concept of magnifier. This magnifier is the ratio of the maximum intensity of moment or shear with transverse cell distortion to that without it.

For reinforced concrete voided slabs, the main problem arising in this method, is the determination of the slab stiffnesses. For an uncracked section, Elliot & Clark (1982), proposed values for these stiffnesses based on a finite element solution for a monolithic section. For a cracked reinforced concrete voided slab, the flexural stiffnesses can be calculated as concrete section cracked due longitudinal bending only, or cracked in both the longitudinal and transverse directions. On the other hand, there is no known method for calculating the torsional inertia of a cracked voided slab, therefore it is assumed constant before and after cracking.

This method is used throughout the research work for the analysis of the tested slabs.

3. EXPERIMENTAL WORK

Six reinforced concrete voided slabs with 10 voids were tested. The dimensions of these slabs are 1.04 x 1.80 m. and thickness 12 cm. These slabs were tested, as simply supported on span of 1.60 m., twice. Once with a single concentrated load acting at center of gravity of the slab within the elastic range, and the second time, with an eccentric concentrated load, of eccentricity 0.3 m. from the center of the mid section. The six slabs were divided into two groups, each group consisted of three slabs;

Group (1) : The three slabs had a bottom reinforcement of 10 \emptyset 6 mm/m' in the longitudinal direction and 10 \emptyset 6 mm/1.5 m' in the transverse direction. The varying parameter was the void's size (For slab S1/6 the void diameter was 63 mm., slab S2/6 the void diameter was 50 mm. and for slab S3/6 the void diameter was 40 mm). The spacing of center line of voids was 0.1 m.

Group (2) : The three slabs had the same void sizes as used in group (1) but the reinforcement used was \emptyset 8 mm instead of \emptyset 6 mm. The slabs were named S1/8, S2/8 and S3/8, respectively.

4. ANALYSIS OF THE EXPERIMENTAL RESULTS

4.1 The centric loading test

In this test all slabs behaved in a similar manner. No cracks appeared during the first test of the six slabs. Good symmetry was observed during these tests and the results showed a good correlation with those obtained theoretically.

4.1.1 Deflections

The experimental results were higher than those obtained theoretically by about 10-20 % as shown in fig. 1 . It was noticed that the deflection decreases as the void's diameters decrease, and also as the reinforcement increases.

4.1.2. Bending moments

During the analysis of the longitudinal bending moments, the cross distribution of this moment is assumed to be similar to the cross distribution of the longitudinal strains in the slab. For the centric loading test, good correlation was observed between the experimental and theoretical results. A better cross distribution of strains was observed for the slabs with smaller void diameter, than those with larger ones, and also this cross distribution improved with the increase of the percentage of reinforcement.

Form the results of deflection and bending moments it is clear that it is essential to include the contribution of steel in calculating the uncracked section inertias.

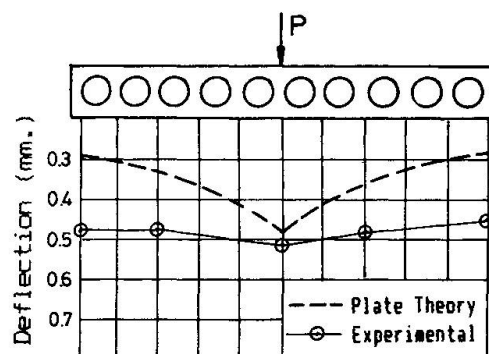


Fig. 1 Deflection distribution along the mid section of slab S1/6 at P = 15 KN (Centric loading)

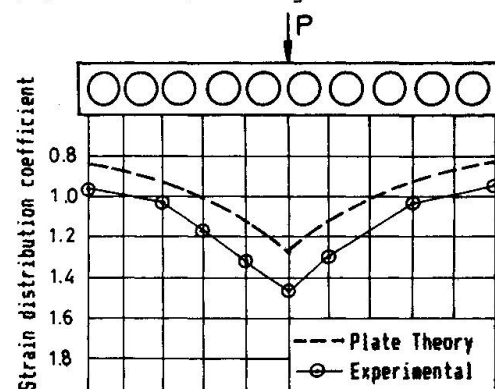


Fig. 2 Strain distribution coefficient along the mid section of slab S1/6 at P = 15 KN (Centric loading)



4.2 The eccentric loading test up to failure

For the six slabs, the first crack appeared at a load of about one quarter of the ultimate load. At higher load levels cracks due to transverse moment and torsion appeared. It was noticed that the cracks appeared earlier in the slabs with smaller percentage of reinforcement, than those with higher ones. Within the same group, cracks appeared earlier in slabs with larger voids, than those with smaller ones. Failure occurred in all slabs due to a combined action of bending and torsion. Slabs of group (1) failed at lower load level than those of group (2), but within the same group the difference between the failure loads was small.

4.2.1 Deflections

The experimental and theoretical distributions of deflections at different stages of loading along the cross section at the midspan of slab S1/6, is shown in fig.3. The experimental results differed from the theoretical ones by about 10-20 % before cracking, and exceeded it by about 20-30 % after cracking. Similar curves are obtained for all six slabs.

A comparison between the load deflection curves, at a point under the load, for all six slabs is shown in fig. 4. From the fig. it is noticed that, as the reinforcement was kept constant, and the void size increases, the deflection values increases. Also as the percentage of reinforcement increases, the deflection value decreases.

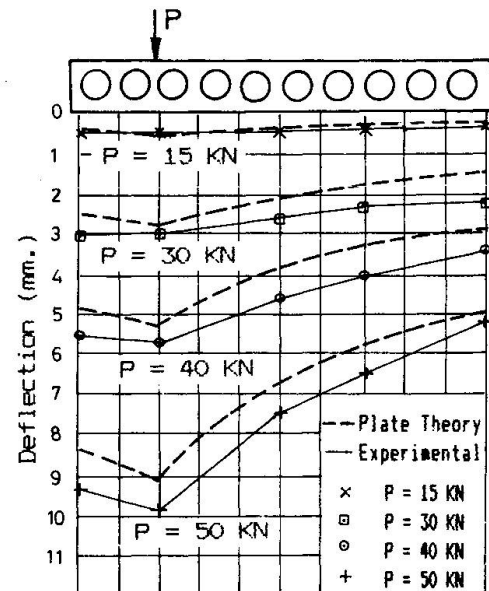


Fig. 3 Deflection distribution along mid section of slab S1/6 at different load levels.

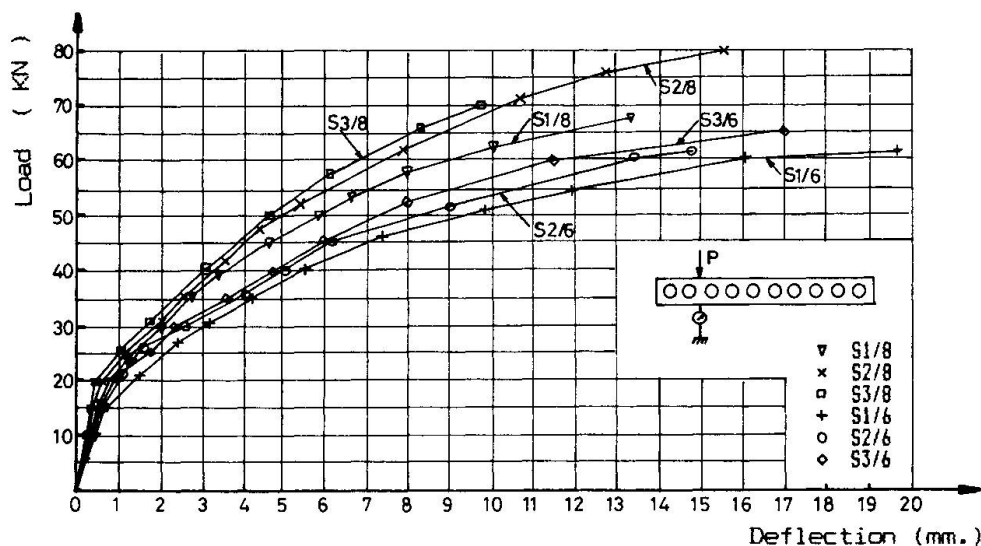


Fig. 4 Load deflection curves of the six tested slabs for a point under the load (Eccentric loading).

4.2.2 Longitudinal bending moments

The strain distribution coefficient across the mid section of the slabs within the elastic range of loading showed a similar correlation with those obtained theoretically, as in the case of centric testing.

Fig. 5 shows the distribution of strains across the slab after cracking. The calculated values of distribution coefficient using inertias of completely cracked section, underestimates the real value. These values are more likely to correlate with those obtained using monolithic section inertias. This is because of the omission of the tension stiffening of concrete in tension between cracks, in calculating the cracked section inertia.

The relation between the strain distribution coefficient and the applied load is shown in figure 6. From the figure the following comments can be concluded;

Before cracking the distribution factors differed by about 15-30% from theory.

After cracking the distribution of the moment improved. This can be explained by that, after cracking the longitudinal flexural stiffness decreases due to the sudden decrease in the sections inertia while the transverse bending and torsional stiffness are approximately constant, and hence the distribution of moment among the webs should improve.

The distribution coefficient, after cracking, for the web under the load, was found to be greater than that obtained theoretically, (using cracked section inertias), but as the load increases this value decreases to converge with the calculated one. This is because, as the load increases, the cracks spread and, the tension stiffening is gradually broken down, causing the distribution coefficients to approach the calculated values.

After the slab began to crack due to transverse moment and torsion, the transverse flexural and torsional stiffness decreased. Consequently, the stresses began to concentrate under the load as shown in the figure.

This behaviour is similar for all the tested slabs, but it was noticed that as the void size decreases the distribution of load improves. Also increasing the percentage of reinforcement improves the load distribution across the section.

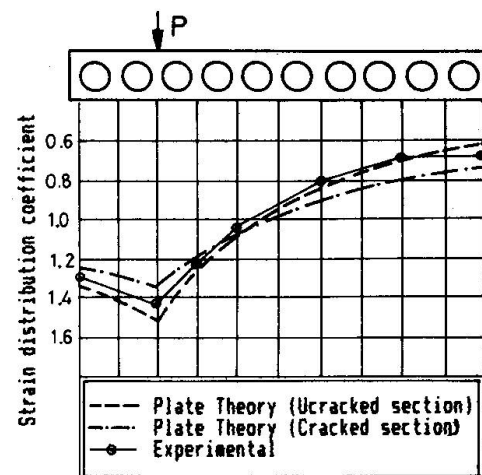


Fig. 5 Strain dist. coefficient across slab S1/6 at $P = 30$ KN.

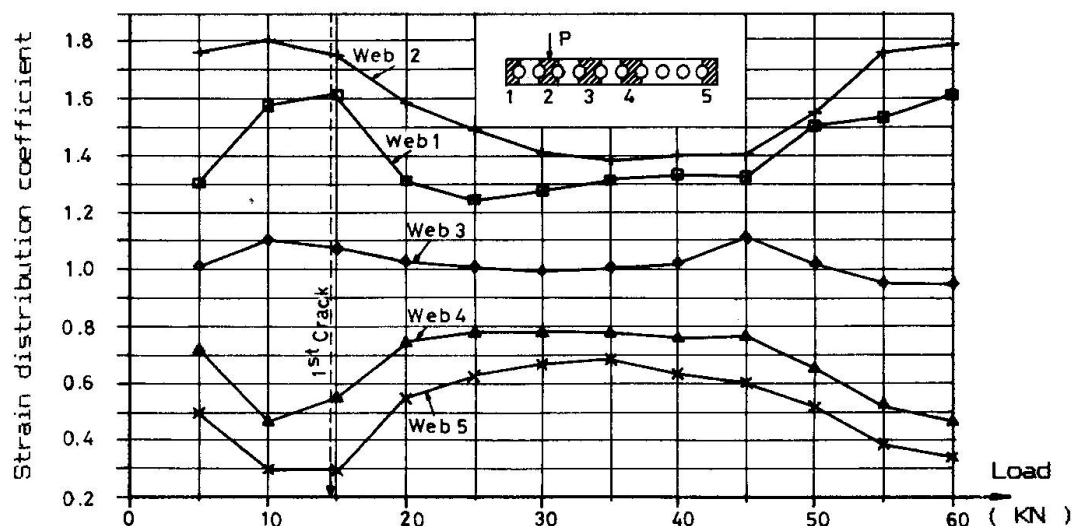


Fig. 6 Variation of strain distribution coefficient with load for slab S1/6. (Eccentric loading)



4.2.3 The transverse moment

The distribution of strains in the transverse steel at mid section of the slab S1/6 is shown in fig. 6. The ratio of the transverse to the longitudinal strains increases as the void-depth ratio increases. This ratio was ranging from 0.1 to 0.16 for slabs S3/6, 0.15 to 0.2 for slab S2/6 and 0.2 to 0.3 for slab S1/6. The same ratios were obtained for slabs S1/8, S2/8 and S3/8.

6. CONCLUSIONS

1. The orthotropic plate theory can be used for the analysis of circular voided concrete slabs with the condition that the stiffnesses of the slab are defined.
2. Decreasing the void-depth ratio improves the load distribution across the voided slabs.
3. Cracking of concrete due to longitudinal moment decreases the stress concentration beneath the loaded web, and hence, the load distribution among the other webs of the voided slab increases.
4. The ratio of transverse to longitudinal moments increases with the increase of the void-depth ratio.

REFERENCES

1. ROWE, R.E., Concrete bridge design. London, CR Books Ltd, 1962. pp. 336.
2. CUSENS, A.R. and PAMA, R.P., Bridge Deck Analysis. London, John Willy & Sons, 1979. pp. 277.
3. MASSONET, CH., and GANDOLFI, A., Some Exceptional Cases in the Theory of Multigrade Bridges. IABSE publications, 1967.
4. CUSENS, A.R., Load Distribution in Concrete Bridge Decks. Construction Industry Research and Information Association CIRIA, Report 53, Dec. 1974. pp. 38.
5. CLARK, L.A., Comparisons of Various Methods of Calculation the Torsional Inertia of Right Voided Slab Bridges. Technical Report 42.508, Cement and Concrete Association, London, June 1975. pp. 34.
6. BAKHT, B., JAEGER, L.G. and CHEUNG, M.,S., Cellular and Voided Slab Bridges. Journal of the Structural Division, Proceedings of the American Society of Civil Engineers. ASCE, Vol. 107. No. ST9, Sept. 1981. pp. 1797-1813.
7. ELLIOT, G. AND CLARK, L.A., Circular Voided Concrete Slab Stiffnesses. Journal of the Structural Division, Proceedings of the American Society of Civil Engineers. ASCE, Vol. 108. No. ST11, Nov. 1982. pp. 2379-2393.

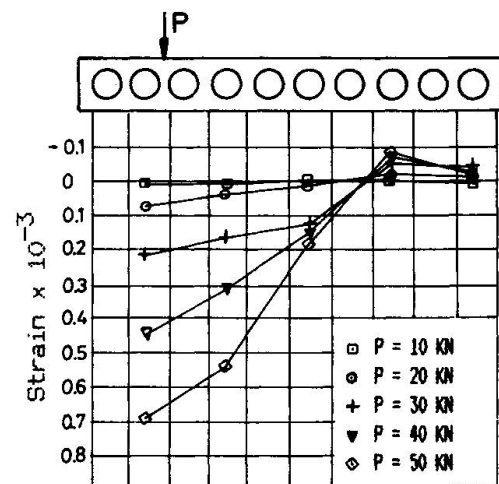


Fig. 7 Distribution of strain in transverse steel of slab S1/6 at different load levels.

Load Carrying Capacity of Steel Tubular Tower Structures

Résistance de tours en ossature d'acier tubulaire

Tragwiderstand von Stahlrohrtürmen

Kelichiro SUITA
Research Associate
Kyoto University
Kyoto, Japan

Kiyoshi KANETA
Professor
Kyoto University
Kyoto, Japan

Isao KOHZU
Associate Professor
Kyoto University
Kyoto, Japan

Sinya INAOKA
Graduate Student
Kyoto University
Kyoto, Japan

Kazuo FUJIMURA
Manager, Dept. Tower Engrg.
Nippon Denro Mfg. Co., Ltd
Kyoto, Japan

SUMMARY

Stability and deformability of ordinary double-Warren truss structures were examined by experimental investigations. The test results show that premature buckling of the compressed members due to end constraints has been observed and the improvement of the durability of structures as a whole cannot be expected in the event of severe loading conditions. A newly developed knee-bracing system has been proposed and improvement in durability of the system was confirmed experimentally.

RÉSUMÉ

La stabilité et la déformation d'un contreventement à double grille ont été étudiés expérimentalement. Les résultats montrent un flambage prématuré des éléments comprimés. Une amélioration de la durabilité de l'ensemble de la structure sous un charge importante ne peut être attendue. Un nouveau type de renforcement aux angles est proposé et l'amélioration de la durabilité est confirmée expérimentalement.

ZUSAMMENFASSUNG

Stabilität und Verformungsverhalten von gewöhnlichen Doppelgitterbalken wurden experimentell erforscht. Als Ergebnis konnte das vorzeitige Knicken der unter Druck stehenden Teile aufgrund des Druckes auf deren Enden beobachtet werden. Weiter zeigte sich, dass im Falle intensiver Belastung keine Verbesserung der Dauerhaftigkeit der Bauten als Ganzes erwartet werden kann. Es wird ein neu entwickeltes Halbdagonalverspannungssystem vorgeschlagen. Die Verbesserung der Dauerhaftigkeit des Systems wurde experimentell bestätigt.



1. INTRODUCTION

This paper refers to stability and deformability of typical double-Warren truss tower structures composed of circular hollow sections, which are widely used in constructing steel tower structures like as electric transmission towers and telecommunication towers. In current design practice, the structures are regarded as being collapsed as a whole, when buckling in a primary compressed member occurs, strength and deformability of the structures are not taken into account in the post buckling range.

In order to improve the durability of the structure, it is desired to design so that buckling of the primary member does not lead to the collapse of the structure, since the structure can resist without the attainment of collapse mechanism, even if the structure would sustain unexpected external forces over the design load.

From this point of view, a method to improve deformability of the structure by adding bending resistant members is proposed. In order to make clear stability and deformability of the proposed structures in comparison with those of ordinary truss structures, an experimental investigation was carried out using subassemblages of truss structure.

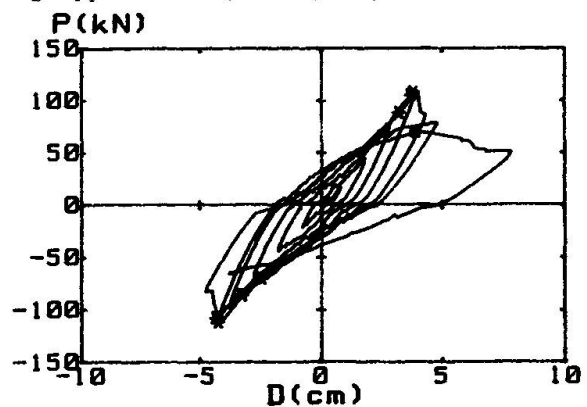
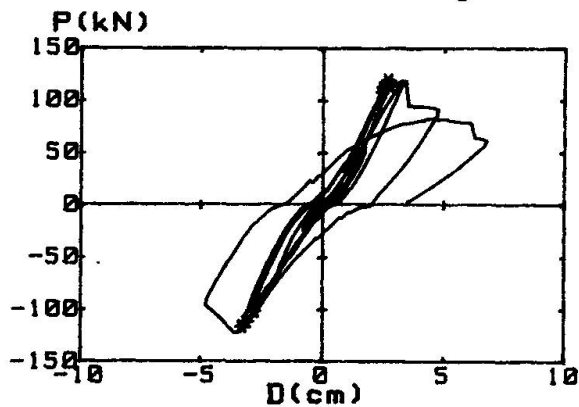
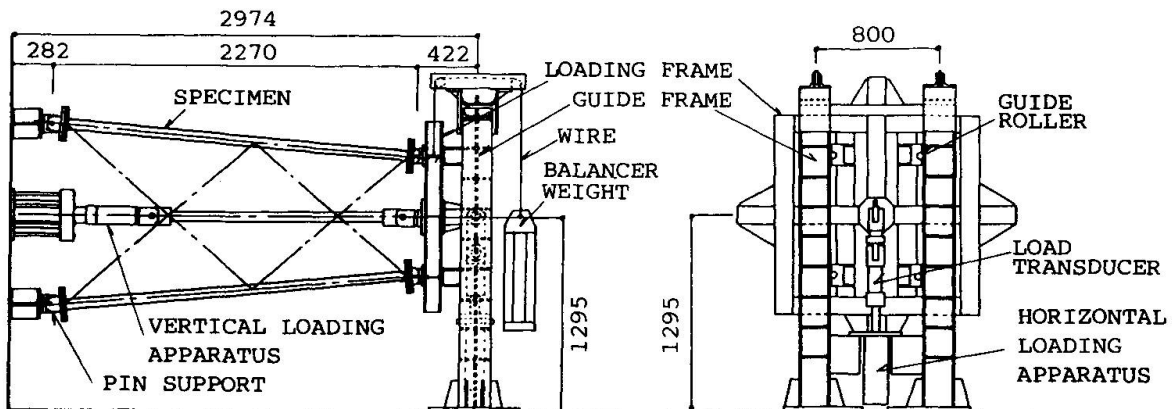
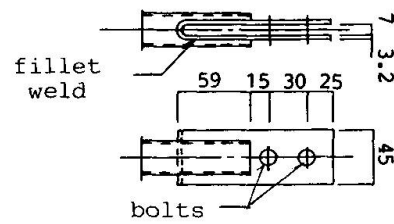
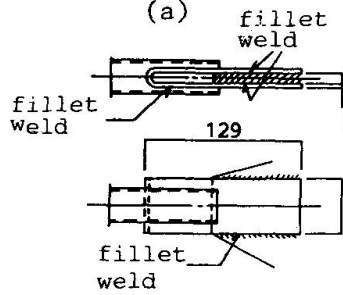
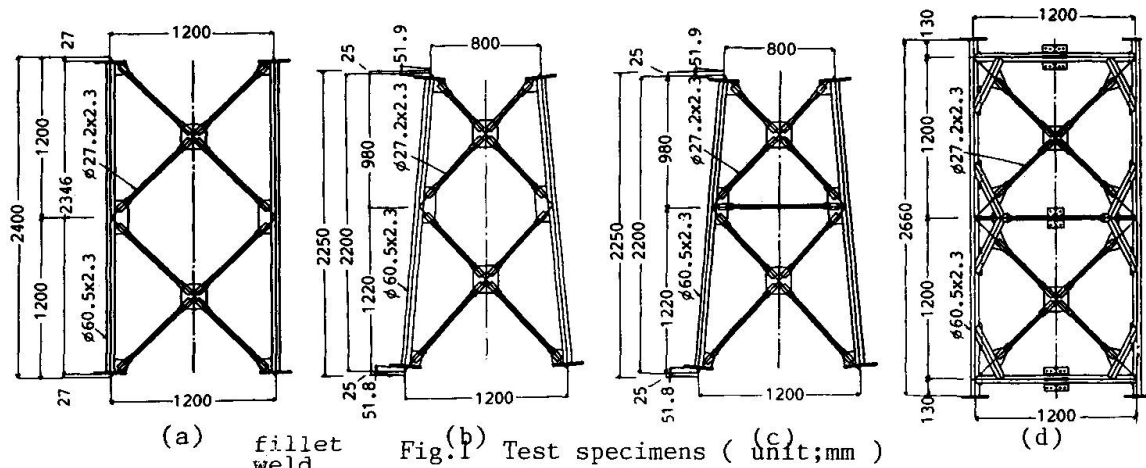
2. EXPERIMENTAL PROGRAM

2.1 Design of specimens

In order to make clear buckling behaviors and restoring force characteristics of ordinary double-Warren truss tower structures, four types of specimens were prepared for the experiment. They were composed of two panels of space truss structures with four legs, and were designed so as to be scaled down about 1/5 of presumed actual truss tower structures rise to a height of over dozens of meters. The structural members were used circular hollow sections made of mild steel. Diameters and thicknesses were 60.5mm, 2.3mm for the leg members, and 27.2mm, 2.3mm for the diagonal members, respectively. Fig.1 shows the side view of the test specimens.

The Type-A specimen (Fig.1a) was designed so that four leg members were arranged parallel to each other and that the angle between the leg members and the diagonal members were 45° . The slenderness ratios of members were 58.25 in leg members and 96.42 in diagonal members, if regarding the distances between the intensity points of element longitudinal axes as the buckling lengths. The joint elements were designed so that all of the axes of members connected to the joint intersected at a certain point without eccentricity. Two types of connecting method, namely, welded and bolted connections, were prepared for Type-A specimens, as shown in Figs.2 and 3. Connecting method of Type-AW was fillet weld, and two galvanized bolts were used for each connection of Type-AB.

Type-B specimens (Fig.1b) had 1/11.25 slant in leg members and the widths of structures were reduced to 80cm at the tops of the specimens. Type-C specimens (Fig.1c) were formed by adding horizontal strut members to Type-B specimens at the center of specimens. The horizontal members were identical to diagonal members. The connecting method of Type-B and C specimens were similar to the method of Type-AB, and all specimens applied bolted connections were galvanized to reflect a phenomenon of slippage as observed in the actual bolted connections. The slenderness ratio of the leg member was 59.22, and the ratio of diagonal member was 102.27. All compressive members were supposed to buckle in the inelastic range, because the slenderness ratios of the members were less than the critical slenderness ratio.





Type-D specimen (Fig.1d) is an example of the improvement to prevent premature buckling of compressive members by adding bending resistant members called as 'Knee brace' to the ends of the diagonal members. The overall dimensions of the specimen were identical to Type-AB specimens except Knee braces. Knee brace members were same as leg members and fillet welded to leg and horizontal strut members. The section and length of Knee brace members were proportioned so that flexural yielding of Knee brace members preceded to buckling of the compressive members.

2.2 Testing Procedure

Fig.4 shows the testing apparatus for horizontal and vertical loadings and the set up of the test specimen. The test specimen was laid horizontally and pin-supported on a reaction wall at the ends of four legs. Rotations were allowed at the supported points. Loads were applied to the specimens by two hydraulic jacks. The horizontal load was applied in two different directions, 0° or 45° (the diagonal direction of the tower section). The applied load was controlled by monitoring the magnitudes of loads and the horizontal displacements of the applied points. Additionally, a constant vertical load was applied to certain specimens. The value N was kept constant at $0.2N_{cr}$ or $0.4N_{cr}$. N_{cr} was four times the buckling load of each leg member which had been calculated from the result obtained by the horizontal loading test.

3. EXPERIMENTAL RESULTS AND DISCUSSIONS

3.1 Effect of Connecting Method on Joints

Fig.5 and 6 show the relations between the applied horizontal load P and the horizontal displacement of the loading point D , obtained from the results of the experiments of Type-A specimens. In the experiments, only horizontal loads in 0° direction were applied. The symbols, '*', illustrated on the loci indicate the occurrence of buckling observed from the records of strains measured by wire strain gauges stucked on each compressive member.

Initially buckling occurred at the diagonal members of the lower panels, and at that time the structures had arrived at the ultimate states. Once buckling occurred, the rigidity and restoring force of subassemblages deteriorated rapidly, and after the subsequent buckling of leg members subassemblages collapsed. These phenomena were commonly observed in both Type-AW and AB.

However, inspite of buckling phenomena, the deformations were remarkably different from each other since the slippage occurred in the bolted connections. In order to assess such deformation characteristic of the bolted connections, the monotonic tensile test was conducted and the result is shown in Fig.7. From the figure, it can be observed that the connection can resist effectively only after the slippage, but the excessive distortion is inevitably generated.

3.2 Effect of Vertical Loads

Fig.8, 9 and 10 show load-displacement relations of Type-B specimens, which were subjected to cyclic loads in the direction of 0° as well as vertical loads in the constant level, namely, $N=0$, $0.2N_{cr}$ or $0.4N_{cr}$.

In the case of no vertical loading, the overall load-displacement relations of Type-B are similar to those of Type-AB, as shown in Fig.8. As the vertical load increased, buckling of primary members occurred in lower level of horizontal load, while reduction of rigidity due to slips of the bolted connections occurred in higher level of horizontal load, and deformability of frame reduced. The experimental results of Type-C specimens indicated similar characteristics.

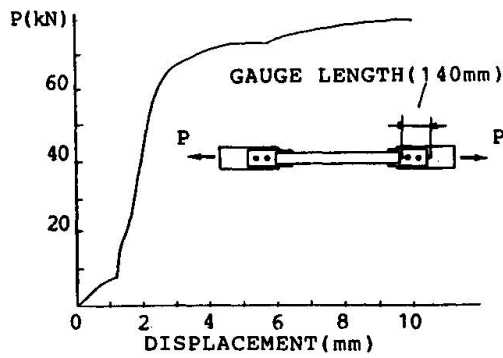


Fig.7 Slip characteristic of bolted connection

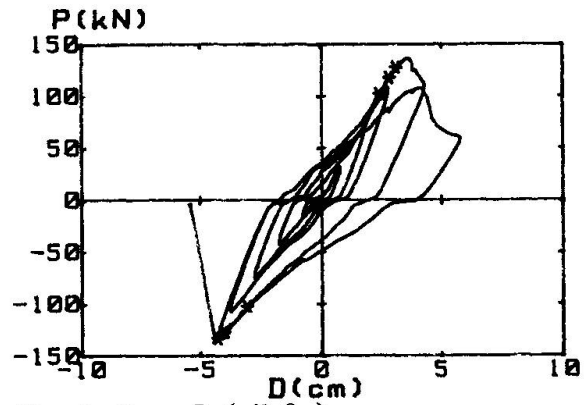
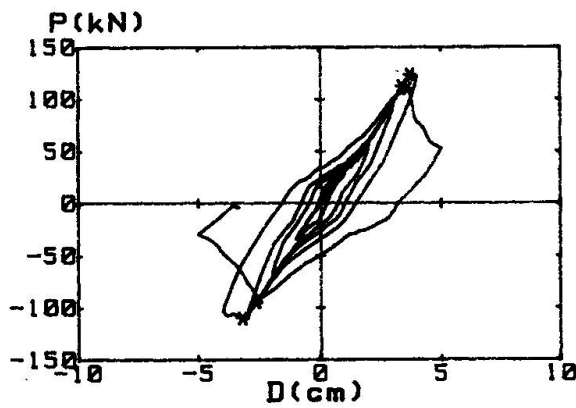
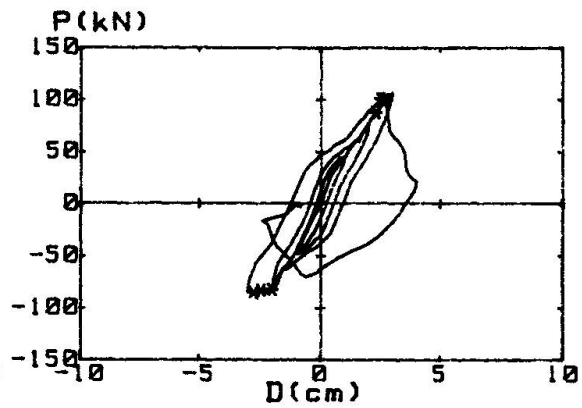
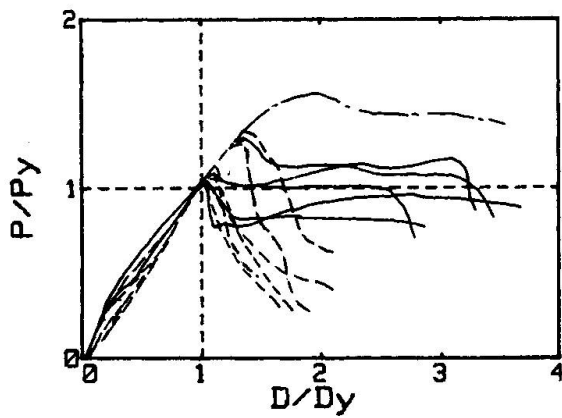

Fig.8 Type-B ($N=0$)

Fig.9 Type-B ($N=0.2N_{cr}$)

Fig.10 Type-B ($N=0.4N_{cr}$)


Fig.11 Normalized P-D relations

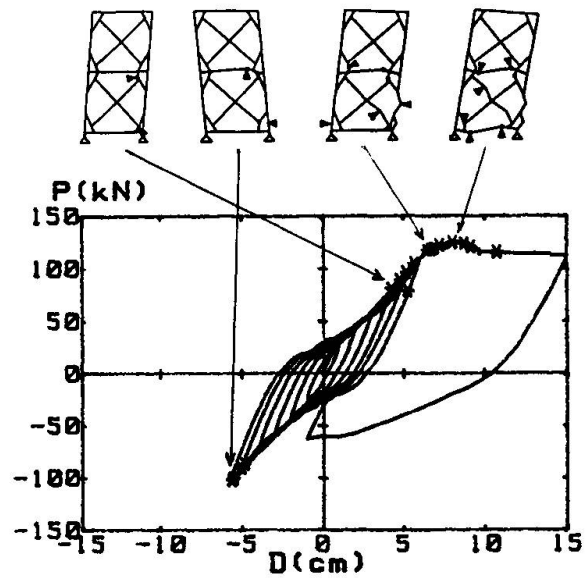


Fig.12 Type-D P-D relation



3.3 Effect of Direction of Horizontal Loads

Fig.11 shows the normalized horizontal load P/P_y - displacement D/D_y relations, where P_y and D_y are the specific load and the displacement corresponding to the initial buckling of each specimen. These lines indicate envelopes of hysteresis loops. Solid lines indicate the results loaded in 45° direction and dotted lines indicate the results of 0° direction loadings. In the case of 45° direction loading, the primary members initially buckled at the compressive leg members, while the restoring force did not deteriorate so sharply, in comparison with the case of 0° direction loading. After buckling of compressive leg member, overturning moment was carried by other three leg members and capacity of the structure as a whole was kept constant at a certain level. From the results, it may be considered that stability and deformability of structures are unreliable especially in 0° direction loading.

3.4 Improvement on Stability and Deformability

Fig.12 shows the horizontal load-displacement relation of Type-D specimen, subjected to the horizontal load in 0° direction alone. The process of failure is illustrated. In the figure, the symbol, \blacktriangle , indicates buckling of compressive members and yielding due to tensile stress or bending moment. Initially, the Knee brace member yielded and then the diagonal members buckled. As the result, the stiffness of the frame reduced, but the restoring force characteristic remained stable without distinct deterioration. The normalized load-displacement relation is shown in Fig.11 by a chain line to compare with other specimens, taking the critical load P_y as the load at the time when a Knee brace member initially yields. From the figure, it can be remarkably observed that higher restoring force and fairly well deformability are exhibited and improvement in reliability and deformability of the structure is confirmed.

4. CONCLUSIONS

From the results of this study, the following mechanical properties of truss space towers subjected to horizontal and vertical loads have been revealed.

- (1) The slippage of joint between the parts connected by bolts causes reduction of the rigidity and the influence of slippage can not be ignored, when considering restoring force characteristics of the structures.
- (2) When horizontal force is applied in 45° direction, the structure can exhibit fairly well deformability, even after buckling primary compressive members. When the horizontal load is applied in 0° direction, load resistant capability deteriorates remarkably after buckling, and neither stability nor deformability of structure is reliable, especially under vertical loads.
- (3) Contribution of newly developed 'Knee bracing system' toward improvement of deformability of truss structure has been confirmed experimentally, and improvement in reliability and durability of the structure is anticipated.

REFERENCES

1. J. Dario Aristizabal-Ochoa, Disposable Knee Bracing: Improvement in Seismic Design of Steel Frames. ASCE Journal of S.E., Vol.112, No.7, July 1986.

Using Fiber Composite Materials for More Durable Concrete Structures

Application des fibres composites pour la solidité des constructions

Anwendung von Faserverbundwerkstoffen für dauerhafte Betonbauten

Reinhard WOLFF

Dr.-Ing.

Strabag Bau-AG

Cologne, Fed. Rep. of Germany



Reinhard Wolff, year of birth 1945. Doctorate at Darmstadt Technical University. Several years in the design office of Strabag Bau-AG, Cologne and Düsseldorf. For the past 4 years head of the central engineering and product management division of Strabag's head office in Cologne.

Hans-Joachim MIESSELER

Dipl.-Ing.

Strabag Bau-AG

Cologne, Fed. Rep. of Germany



Hans-Joachim Miesslerer, year of birth 1944. Studied at Wuppertal University. From 1967 in the design office of Strabag head office in Cologne, since 1987 manager of the department research and development in the central engineering and product management division.

SUMMARY

In recent years heavy-duty composite materials have proven their applicability in numerous constructions as a corrosion resistant alternative to conventional prestressing steel. This will be demonstrated in the following paper by way of three different constructions. These are the Marienfelde Bridge in Berlin, the braced arched tunnel vaulting in Paris and the prestressing of a three span road bridge in Leverkusen. All of these constructions are in turn equipped with sensors in order to minimize the maintenance costs of controlling the constructions, and in order to increase the durability of the constructions by utilizing composite fibre materials for the prestressing tendons.

RÉSUMÉ

Les fibres composites ont fait leur preuve dans de nombreuses constructions en tant qu'alternative anti-corrosion à l'acier de précontrainte. Trois réalisations illustrent cette application: le pont Marienfelde à Berlin, le haubannage horizontal d'un tunnel du Métro à Paris et la précontrainte d'un pont à Leverkusen à trois travées. Toutes ces constructions sont équipées de capteurs pour faciliter les travaux de contrôle et de fibres composites pour les câbles précontrainte afin d'améliorer la solidité des constructions

ZUSAMMENFASSUNG

Inzwischen haben sich Hochleistungsverbundwerkstoffe als korrosionsbeständige Alternative zum herkömmlichen Spannstahl an zahlreichen Bauwerken bewährt. An drei verschiedenen Bauwerken wird dies im folgenden Aufsatz dargestellt. Es sind dies die Brücke Marienfelde in Berlin, die Abspannung eines Tunnelgewölbes in Paris und die Vorspannung einer dreifeldrigen Strassenbrücke in Leverkusen. Alle Bauwerke sind wiederum mit Sensoren ausgerüstet, um den Wartungsaufwand für die Kontrolle der Bauwerke zu minimieren und durch die Anwendung von Faserverbundwerkstoffen für die Spannglieder, die Dauerhaftigkeit der Bauwerke zu steigern.

1. THE BRIDGE "BERLIN-MARIENFELDE"

A leisure park has been created during the past few years on the site of an earlier refuse depot in Marienfelde, Berlin. This park and a protected landscape area located to the south of the site were to be linked by a public footway. Industrial railway tracks, which separate the two areas from one another, necessitate the construction of a pedestrian bridge (Fig.1) which can also be used by riders and ambulances. During the design work by the Senator for Construction and Housing, it was agreed with Berlin Technical University to use the bridge as a research project for the purpose of study and for the application of new design concepts. The bridge's outline design provides for a 5 meter wide, two span, slab-and-beam bridge with spans of 27.61 mtrs. and 22.98 mtrs. The bridge superstructure has an overall height of 1.10 mtrs. and will be executed for the first time in Germany with a partial prestressing having externally arranged prestressing tendons without bond. The prestressing tendons, a new development by STRABAG BAU-AG, consist of composite fiber materials (glassfibers embedded in a resin matrix) with integrated optical fiber and copper wire sensors for the continuous monitoring of the bridge.

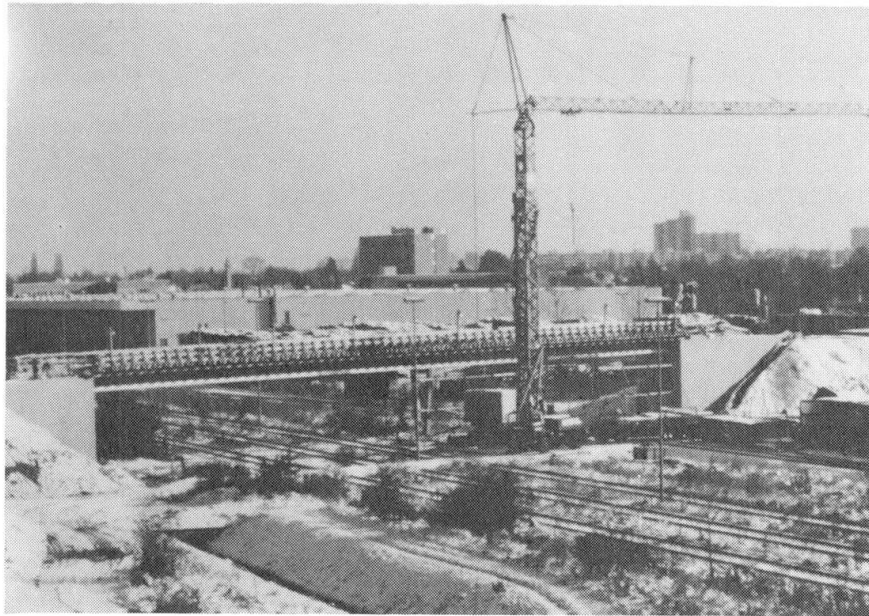


Fig. 1 Bridge Berlin-Marienfelde

1.1 THE PRESTRESSING TENDONS

The utilization of heavy duty composite materials; the future generation of prestressing tendons for concrete structures.

Following the completion of two bridge structures in Düsseldorf, prestressing tendons are again being employed which are composed of individual glassfiber bars. These glassfiber bars, manufactured by BAYER AG under the brandname (R)Polystal, have a diameter of 7,5 mm and comprise of 60.000 glass fibers which are strictly orientated in one direction.



A total of 19 if these glassfiber bars form one prestressing tendon which is supported against the concrete by means of in-situ-grouted anchors developed by STRABAG BAU-AG. The bar material is a further development of the prestressing tendons on the Ulenbergstraße Bridge in Düsseldorf. The innovation in this case is, however, the external application of the prestressing tendons. The tendons (Fig.2) run externally between the two main bridge beams, around each of two transverse beams in the bay sections and then upwards along the central colum over the transverse beam (Fig.3). Since the prestressing elements are accessible at all times, they can easily be checked and, if necessary, replaced. This means a bridge design which is easy to maintain.

Fig. 2 External application of the prestressing tendons

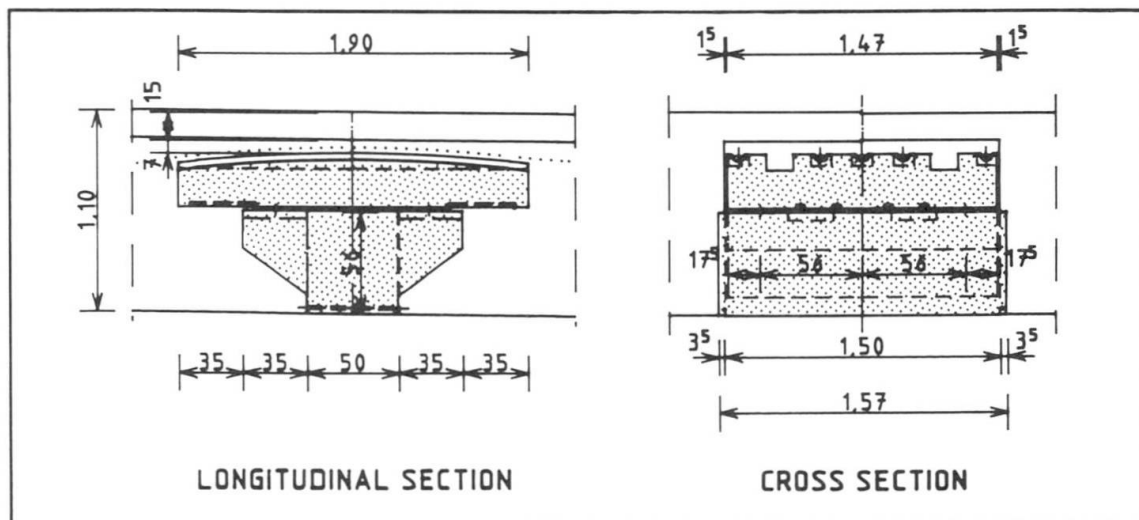


Fig. 3 Diversion support for the prestressing tendons

1.2 LOADING TEST OF THE BRIDGE

In order to be able to study precisely the loadbearing behaviour of the bridge's design, the bridge is subjected to an imposed load of 1.5 times the live load (7,5 KN per sq.mtr.). The load is simulated by means of a total of 250 pieces of reinforced concrete slabs (weight of each slab 10 KN) having a total load of 2500 KN. The deflexion of the bridge spans, the bearing forces, prestressing tendon forces and the strain on the steel concrete reinforcement were measured.

2. BRACING UP OF ARCHED TUNNEL VAULTING

The abutment strength of a station's vaulting has decreased unilaterally due to a construction pit located in the vicinity of this subway station in Paris. Thus, a prestressed tie rod has to be built in order to prop up the vaulting (Fig. 5).

The abutment for the tie rod consists of steel anchors cast in-situ into the vaulting's supports. The tie rod itself consists of 36 composite glass fiber prestressing tendons with a working load per prestressing tendon of 650 KN.

The client decided on the employment of composite fiber materials for the following reason.

- electromagnetic neutrality
- excellent resistance in aggressive media
- controllability by means of integrated optical fiber sensors
- low specific weight (hence less supports required for the prestressing tendons).

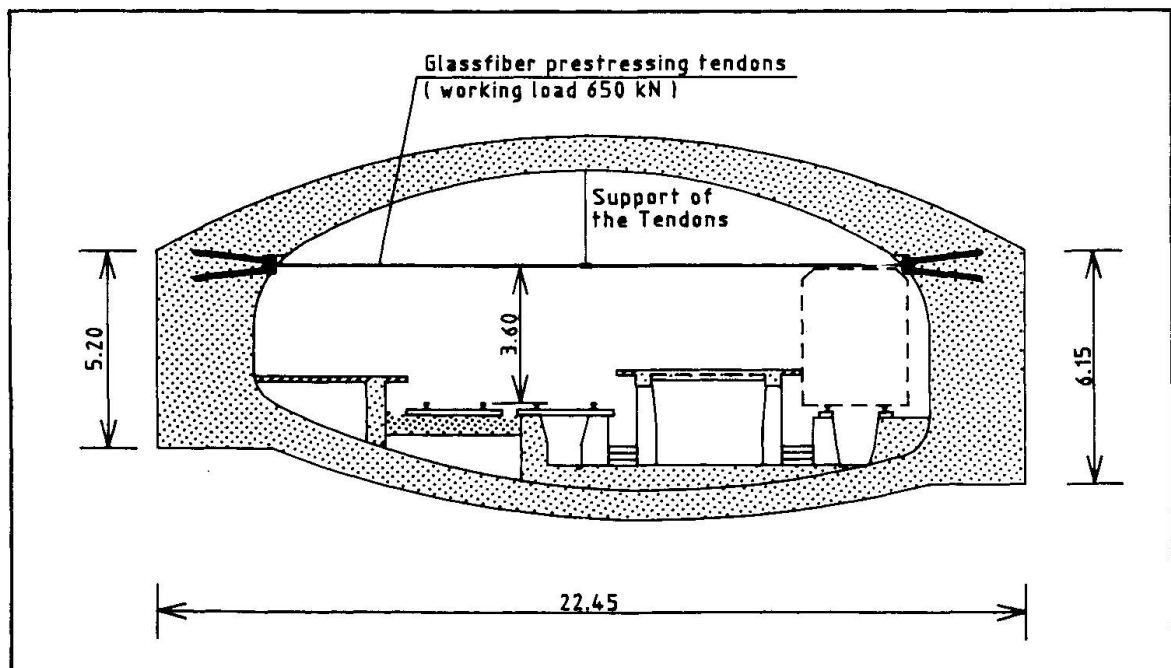


Fig. 4 Cross section of the subway station in Paris

3. TRIPLE SPAN ROADBRIDGE

This triple span road in Leverkusen crosses the entrance to a multi-storey carpark of Bayer AG (Fig. 5).

The spans amount 16,30/20,40/16,30 mtrs. The cross section of the bridge superstructure has a height of 1,10 mtrs., a width of 9,70 mtrs. and is a solid slab beam construction. Limited prestressing is applied. The bridge category is 60/30. The prestressing tendons consist of glassfiber composite bars with integrated sensors. The concrete structure is also monitored by optical fiber sensors surface installed on the concrete after construction.

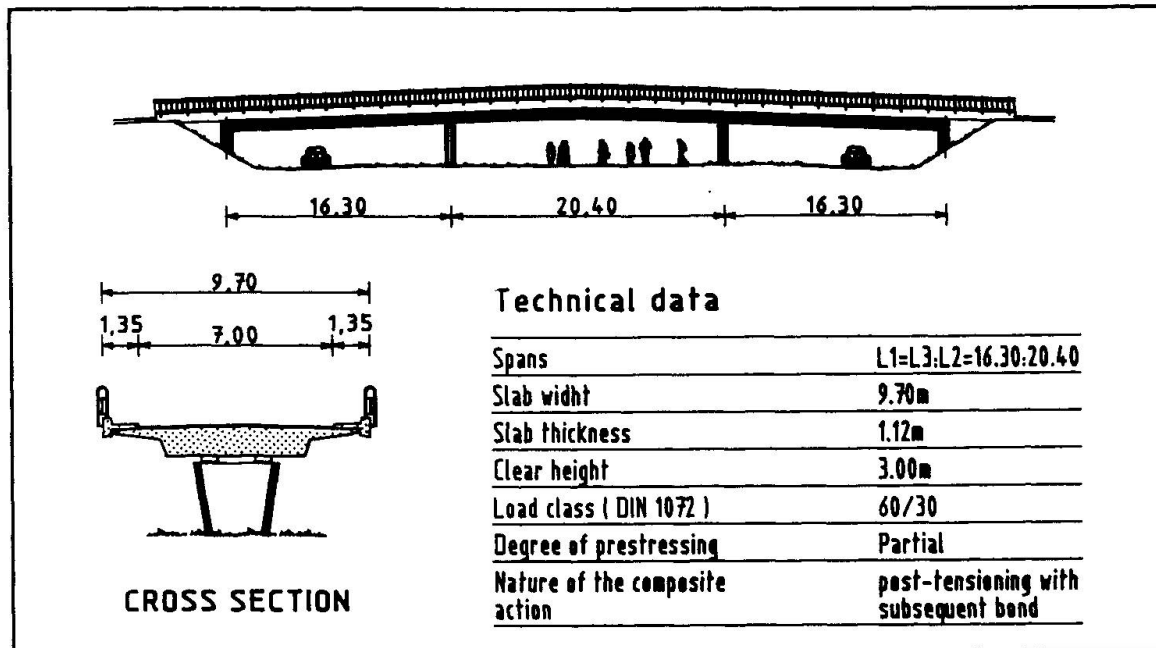


Fig. 5 Triple span roadbridge

REFERENCES

- [1] KALLEJA, H., STAUCH, M., Im Süden Berlins Bau einer Forschungsbrücke, Forschung Aktuell 4, 1987, Nr. 16-17, S. 43 ff
- [2] KÖNIG, G., WOLFF, R., Hochleistungs-Verbundwerkstoff für die Vorspannung von Betonwerken, Bericht zum IABSE Symposium, Paris-Versailles 1987
- [3] WAASER, E., WOLFF, R., Ein neuer Werkstoff für Spannbeton, Beton 36 (1986) H. 7, S. 245-250
- [4] LEVACHER, F.K., MIESSELER, H.-J., Spannkraftmessung mit integrierten Lichtwellenleitersensoren, Bericht zum IABSE Kongress, Helsinki 1988
- [5] FRANKE, L., WOLFF, R., Einsatz von Hochleistungsverbundwerkstoff im Spannbeton Brückenbau, Bericht zum IABSE Kongress, Helsinki 1988
- [6] MIESSELER, H.-J., PREIS, L., Hochleistungsverbundstäbe aus Glasfasern als Bewehrung im Beton- und Erdbau, Bauen mit Kunststoffen, H. 2/1988, S. 4-14

Leere Seite
Blank page
Page vide

Fatigue Resistance of a Steel Railway Bridge

Résistance à la fatigue d'un ponts-rail

Ermüdungswiderstand einer Eisenbahnbrücke

Philippe VAN BOGAERT

Dr. in applied sciences
Belgian Railway Co.
Brussels, Belgium



Philippe Van Bogaert, born 1951, graduated in civil engineering at RUG — Ghent University in 1974, and PhD in appl sc RUG in 1987. For one year he was assistant at Ghent University, and since 1977 he is employed by SNCB's Bridge Department, and largely concerned with the design of both steel and concrete railway bridges.

SUMMARY

The paper describes different designs and optimization of a tied arch railway bridge. The design criterium for fatigue damage due to the several loading spectra, was chosen to be the spectrum corresponding to the largest local stress variation. In the case of a completely optimized structure, fatigue resistance becomes more limiting than ultimate limit state of load-carrying capacity.

RÉSUMÉ

Différents projets, ainsi que l'optimisation d'un pont-rail en bowstring sont décrits. Le critère du dommage causé par la fatigue due aux différents spectres de chargement, est choisi en fonction de la variation de contrainte locale maximale. Dans le cas d'une structure totalement optimisée, la résistance à la fatigue est un critère plus contraignant que l'état limite ultime de résistance.

ZUSAMMENFASSUNG

Dieser Beitrag beschreibt verschiedene Entwürfe und die Optimierung einer Stabbogen-Eisenbahnbrücke. Als Bemessungsbedingung wurde aus verschiedenen Ermüdungslastfällen derjenige mit dem grössten lokalen Spannungsunterschied ausgewählt. In einem vollständig optimierten Tragwerk wird die Ermüdungsfestigkeit und nicht die Tragsicherheit massgebend.



1. INTRODUCTION

Prevention of fissuration by fatigue is important, especially in the design of steel bridges that are to support large live loads. The numerous fatigue design codes [1] [2] are concerned with the analysis of fatigue details, which are mostly due to the welding of the bridge-elements. Therefore these details are only known at the actual construction stage. Hence, the designer has to estimate fatigue damage, aiming to avoid, but not being fully able to exclude all fatigue-sensitive construction details.

While designing the railway bridges at Landegem (Belgium), it seemed possible, with moderate success, to account for fatigue, and to draw some conclusions concerning stress limits to adopt. The tied arch bridges that are discussed further were built to suppress a local narrowing in the deviation canal of the river Lys. First two single track bridge decks are constructed on both sides of an existing bridge, the latter being replaced afterwards by a double track bridge.

2. BRIDGE DESIGNS

Different solutions were examined for the superstructure. Among them, the first classical solution consisted of the construction of two pillars on both future canal shores, supporting a central steel bridge deck with 4 m high plane web girders. Two side spans of steel-concrete girders would complete the bridge. For various reasons, such as the presence of existing buttress-walls at the location of the piles, it was decided that three 86 m one-span steel decks were to be preferred. From experience-exchange with Deutsche Bundesbahn [3], the construction of tied arches with vertical suspension hangers was examined (fig.1). A prelimi-

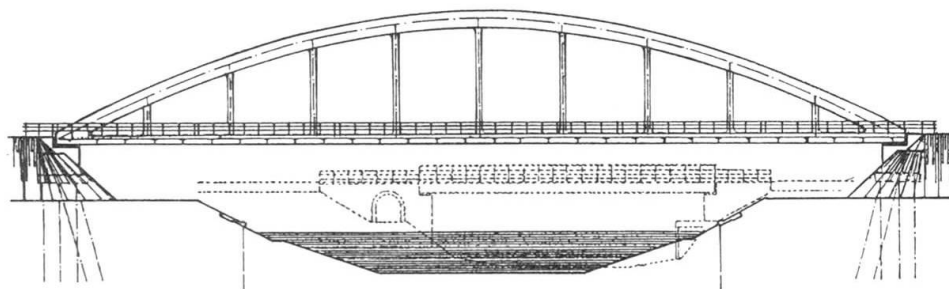


Fig 1 Tied arch with vertical suspension hangers

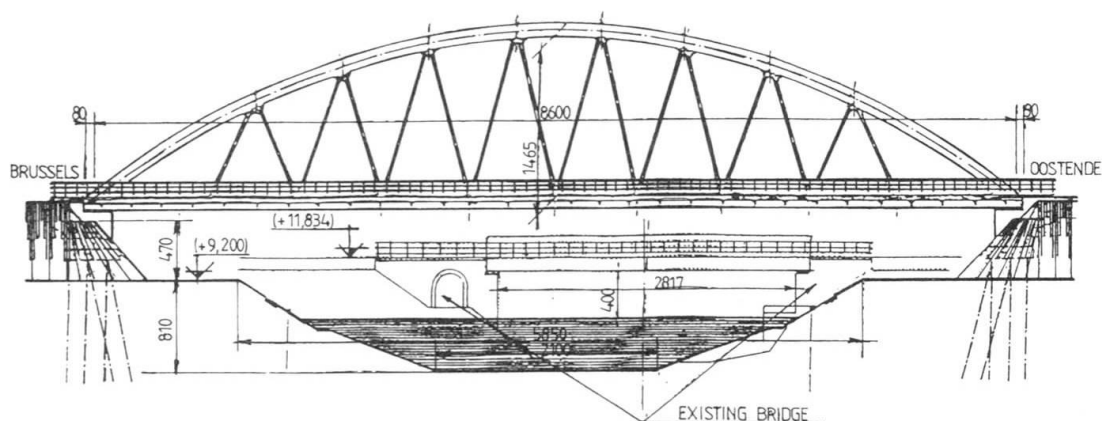


Fig 2 Triangulated hangers

nary analysis, based on the principles that are emphasized further, showed that total weight of construction steel for the three bridges would be about 1455 tons

the deflections caused by the loading by the scheme UIC [4] being $1/995$ of the span. An important improvement (fig.2) was made by disposing the suspension hangers between arches and tie-deck as triangles. Mainly due to the reduction of the bending moment-sum to be distributed between arch and deck [5], total weight of construction steel was now found to be 1275 tons, the deflections being $1/1260$ of the span. However, certain loading cases show that, as the live loads represent some 70% of total loading, and as they induce compression forces in the hangers, the latter are submitted to a maximum residual compression of 221 kN.

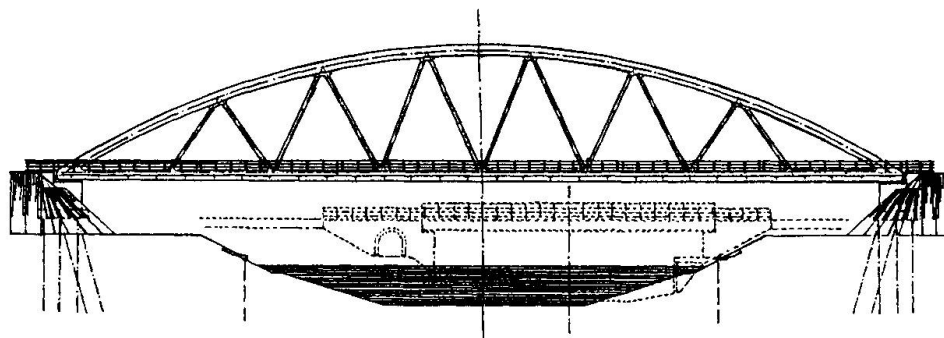


Fig 3 Further improvement of triangulated hangers tied arch

Eventually, the shape that was constructed (fig.3), a further improvement, had a total weight of 1120 tons, maximum deflection of $1/1824$ of the span, and maximum residual compression in its hangers of 291 kN. However, it appeared that stress variations, as well as total safety to ultimate limit state, are distributed quite unequally along the bridge's span, the differences being about 35%.

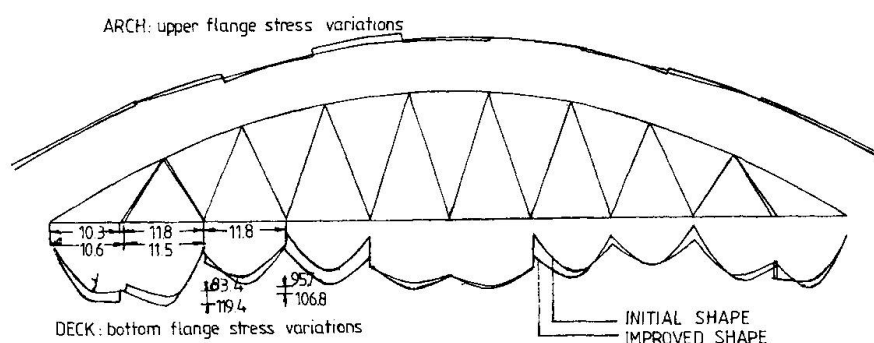


Fig 4 Reducing of stress fluctuations by optimizing

A closer optimizing of the case of a 115 m span bridge, showed that little modifications enabled to reduce stress variations and total safety fluctuations along the bridge's deck and arch's axis, to only 16% (fig.4).

3. FATIGUE STRESSES

All designs were calculated with the UIC loading scheme. The loading spectra to be adopted for fatigue verification, meaning the number of loading cycles, that guarantee a safety of 2.5 for a 50 years lifetime, depend on the influence length of each element, and were determined from UIC-leaflet 778 [2]. In this method, all spectra are reduced to the reference number of $2 \cdot 10^6$ cycles, by modifying the allowable amplitude of stress variations, applying Wöhler's curve with an exponent of 3.75. The procedure is equivalent to ECCS's, the sequence of calcu-



lations being reversed. For design purpose, it was assumed that the determining spectrum for the deck's main girders, corresponds to an influence length equal to the distance between suspension nodes. These girders consist of flange plates welded to webs, to which are again welded the webs of transverse stiffeners. Consequently they belong to ECCS-class 112. Using Wöhler's curve, the allowable stress variation for the adapted design spectrum becomes $\Delta\sigma_{AD} = 125 \text{ N/mm}^2$. Hence, during design the additional local bending between transverse deck stiffeners and the overall extension of main girders were disregarded.

In a similar way, it was assumed that the arch's box section (ECCS-class 100) spectrum corresponds to the total arch length, thus disregarding any local variation due to suspension node's reactions. Both assumptions were found to be

design	1	2	3
arch $\Delta\sigma$ (dam.)	151.2 (1.345)	136.1 (0.899)	78.67 (0.115)
deck $\Delta\sigma$ (dam.)	123.2 (0.947)	102.3 (0.472)	114.9 (0.729)

Table 1 Stress variations and damage

accurate since, after complete analysis of each structure the stress variations (in N/mm^2) from table 1 were found, the numbers between brackets being the total fatigue damage due to all stress spectra.

Table 2 summarizes the values of δ_m , the material's partial safety factor for ultimate limit state, that was determined for both cases of steel quality Fe37 and Fe42.

design	1	2	3
Fe37 deck	1.050	0.942	0.914
arch	1.017	0.868	1.319
Fe42 deck	1.290	1.183	1.147
arch	1.249	1.090	1.655

Table 2 Safety factor u.l.s.

As can be seen from table 2 Fe42 had to be used in the final design. However as it was emphasized in member 2, a more accurate choice of the deck's sections lengths would have permitted the use of Fe37, thus making predominant the criterion of fatigue.

More important fatigue details are present in the shorter elements of the bridge deck, namely the orthotropic plate with closed section stiffeners. Evidently, obtaining the same safety for an equal lifetime, will submit these elements to a

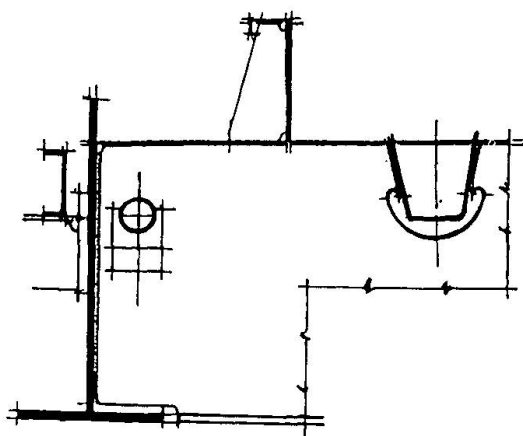


Fig 5 Main girder and continuous closed section stiffener

many larger number of loading cycles. The stiffeners have delicate welding details, such as the joining of their webs with the deck plate (joint I), and the continuous passage through the transverse stiffener's web (joint II). The latter was shaped as a cardioid [6] to avoid stress concentration. The welding length of joint II is determined by the allowable stress variation amplitude. Both joints I and II belong to ECCS-class 80, the local spectrum allowing a stress variation of 60 N/mm^2 . During design it was assumed that the local bending stress variation spectrum is predominant. A full analysis showed the damages summarized in table 3. Hence, although there appears some greater importance of the local spectrum, the contribution of damage due to general effects cannot be neglected.

joint	local bending	general bending	total damage
I	64%	24%	88%
II	31%	21%	52%

Table 3 total damage closed stiffener joints

scale specimen of the orthotropic deck plate was tested on fatigue. A sample, shown in fig.6, of 3.6 m length, consisting of a deck plate with 2 closed section stiffeners, was submitted to pulsating bending. In all critical details strain gages were attached. A stress variation of 60 N/mm^2 was realized in these points.

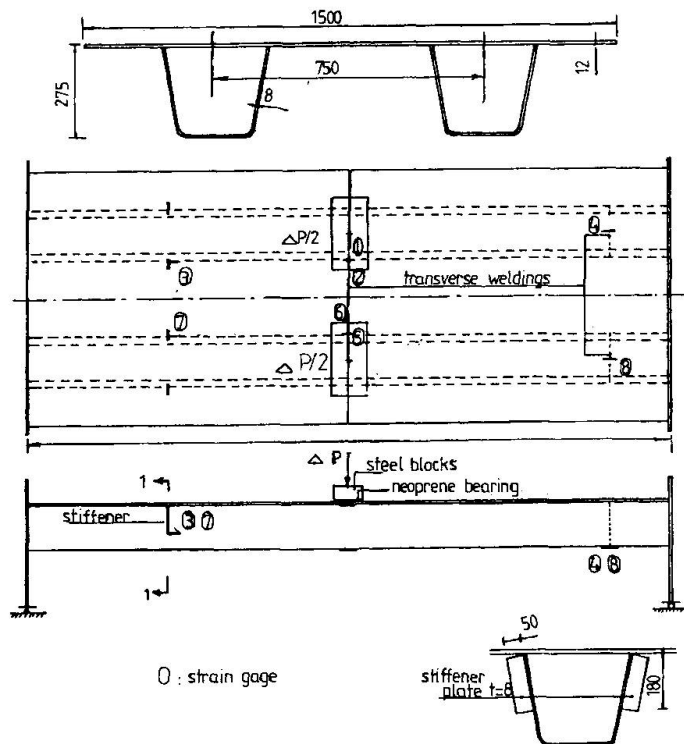


Fig 6 Fatigue test

Consequently, the design values for the local spectrum have to be chosen very low. In the case that was discussed 60 N/mm^2 proved to be an accurate choice.

4. FATIGUE TEST

In order to verify the welding quality and the accordance with theory, a 1/1

Transverse weldings were present and the passage through the transverse girder's web was simulated by the welding of stiffening plates 8 mm of thickness. Stresses' variations went up to 160 N/mm^2 at the mid-section's bottom. As the test was performed at constant amplitude, and since the critical spectrum of an element of 3.6 m is far beyond the damage limit, no fissuration whatsoever might appear. Since, according to ECCS, beyond $5 \cdot 10^6$ cycles no damage does occur, a safety of 1.5 was adopted, the test was stopped after $7.5 \cdot 10^6$ loading cycles. No damage or fissuration was detected after this test.

5. CONSTRUCTION

This paper does not deal with the actual construction of the three bridges. However, it should be mentioned that the bridges

were assembled by placing first the decks, followed by the arches, to which the suspension hangers were already bolted. The gaps between the deck's nodes and hangers, due to the deflection caused by self-weight, were compensated by regulating the level of temporary bearings on construction towers.

One of the completed single-track bridges can be seen from photo 1. As yet, a testing programme for the completed bridges has not taken place. In the future some interesting data may be expected from it.

6. CONCLUSIONS

It was implied that, while designing even moderate sized steel railway bridges,



Photograph 1 Completed single-track bridge

fatigue resistance plays an important role.

Accurate use of verification codes, based on the most wide spectra enables to choose the allowable stress variations for different bridge elements. In those cases where optimized structure geometry has been achieved, prevention of fissuration caused by fatigue, becomes a more strict criterion than ultimate carrying capacity at limit state.

REFERENCES

1. ECCS Recommendations for the fatigue design of steel structures. ECCS, may 1985.
2. UIC Leaflet 778-1 R Recommandations relatives aux facteurs de fatigue à considérer lors du dimensionnement des ponts métalliques de chemin de fer 1st Ed Union Internationale des Chemins de Fer, jan 1981
3. KONRATH H. u JANCKE K., Stählerne Eisenbahn-Stabbogenbrücke über den Main in Frankfurt-Niederrad. Bauingenieur 54 1979
4. UIC Leaflet 702-0 Schéma de charges à prendre en considération dans le calcul des ouvrages sous rail sur les lignes internationales 3d Ed. Union Internationale des Chemins de Fer, jan 1976
5. VIRLOGEUX M. et al, Le pont-rail du Moulin (Nord). Travaux, oct 1984
6. HAIBACH E. u PLASIL I., Untersuchungen zur Betriebsfestigkeit von Stahlleichtfahrbahnen mit Trapezhohlsteifen im Eisenbahnbrückenbau. Der Stahlbau, sept 1983

Design Model for Damaged Concrete Pipes in the Ground

Modèle de calcul de buses détériorées dans le sol

Rechenmodell für Betonrohre im Boden

J. P. STRAMAN

Scientific Staff Member
University of Technology
Delft, The Netherlands



J. P. Straman, born 1938, was for 15 years employed at a consulting firm of design in the concrete structures. Now he is a scientific staff member and involved in studies concerning maintenance and repair of concrete structures.

SUMMARY

Chemical attack on concrete pipes decreases the thickness of the walls unequally, which influences the internal distribution of the forces. To determine the remaining load bearing capacity of the pipes, a design model has been developed. Deflection has been chosen as the new assessment criterion. The permissible deflection depends on serviceability requirements, mainly leakage. With reference to this criterion the loads on the pipe and the strength of the pipe have been determined. A guideline is given to establish the remaining life expectancy.

RÉSUMÉ

Par l'attaque chimique de buses en béton l'épaisseur de la paroi diminue inégalement, ce qui influence des efforts intérieurs. Pour déterminer la résistance à la rupture des buses, un modèle de calcul a été développé. Comme critère de comparaison on a choisi la flexion. La flexion admissible dépend des exigences d'emploi: principalement le coulage. Sur la base de ce critère, les sollicitations sont déterminées et la résistance des buses est contrôlée. Des directives sont données pour déterminer la durée de vie des buses détériorées.

ZUSAMMENFASSUNG

Chemische Beeinträchtigung von Betonrohren im Boden vermindert die Wanddicke ungleichmässig, womit die innere Kräfteverteilung beeinflusst wird. Um das Tragvermögen von beschädigten Rohren festzustellen, ist ein Rechenmodell entwickelt worden. Für das Beurteilungskriterium wurde die Durchbiegung gewählt. Die zulässige Durchbiegung hängt von den Gebrauchsanforderungen ab, hauptsächlich von der Leckage. Mit Bezug auf dieses Kriterium werden die Belastungen auf die Rohre und die Festigkeit des Rohres bestimmt. Zur Ermittlung der Restlebensdauer sind Hinweise gegeben.



INTRODUCTION

The sewerage is an important part of the civil infrastructure: both as function and as replacement value.

Still the maintenance of, and the care for the sewerage have not been in proportion to this great importance.

However by the increasing interest in the field of the environment but also as a result of recently established damage, the interest in technical and economical aspects of the sewerage is growing.

A number of these cases of damage is owing to deterioration of concrete sewer-pipes.

The thickness of the walls of the pipe decreases (depending on the appearing mechanism above or below the waterlevel), resulting in a decrease of the strength and rigidity.

To establish the remaining strength, the existing design methods cannot be used because the pipe is not longer axial symmetrical and besides the design assessment criteria of concrete pipes are not applicable to damaged pipes. In many cases e.g. the pipes are already cracked.

Therefore the Delft University of Technology has, in coöperation with D.H.V. Consulting Engineers Amersfoort, developed a design model for damaged pipes in the ground to establish the remaining strength, whereby another assessment criterion has been applied [1].

DETERIORATION

Biogenic Sulphuric acid Attack (BSA) of concrete is the dominant material degradation process in sewers [2]. Because sulphuric reacts with the cement, concrete loses cohesion,

resulting in a decrease of the thickness of the pipe wall. This deterioration takes place - as opposed to other mechanism - above the water-level and is not uniformly distributed along the inside of the pipe. As approximate guide values for the deterioration at the top and the water-level are given 1,5 times respectively 2,5 times the mean value [3]. See figure 1.

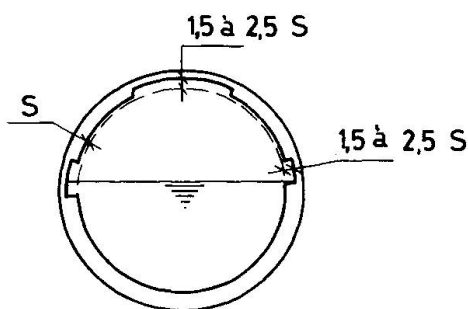


Fig. 1 Schematization of the deterioration of the pipe-wall

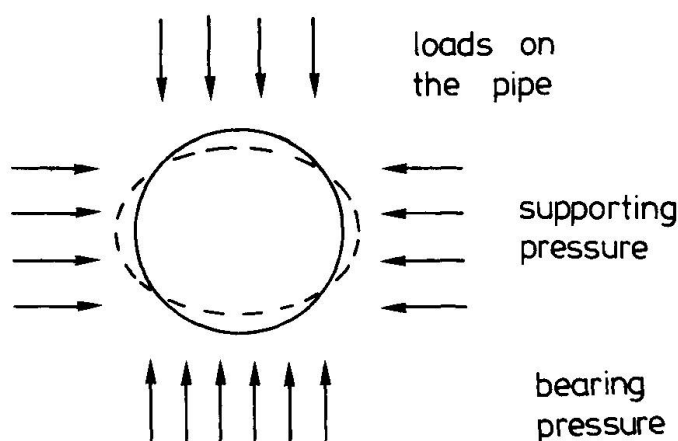


Fig. 2 Behaviour of a relatively flexible pipe

The decrease of the thickness of the pipe-wall has two effects: the pipe is getting less rigid and less strong.

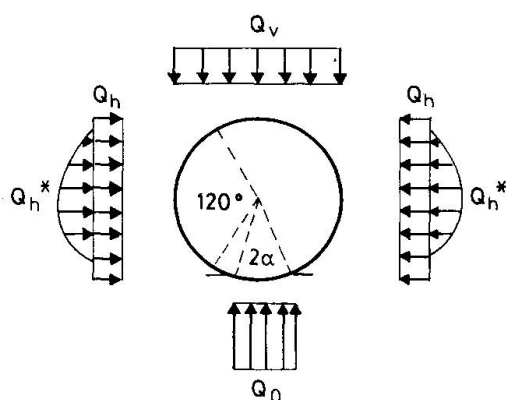
By the first effect the pipe deforms, the surcharge decreases and the horizontal supporting pressure increases. Generally speaking a decrease of the rigidity causes a more favourable distribution of the loads (figure 2). By the second effect the loadbearing capacity decreases.

LOADS ON THE PIPE

The loads on the pipe are determined with the method of Leonhardt as described in [4].

Considered are:

- earth load;
- live load;
- selfweight of pipe;
- pipe filling;
- internal and external pressure;
- temperature differences.



The schematization of the external loads is given in figure 3, where:

Q_v = vertical load

Q_h^* = horizontal supporting pressure, as a result of the deformation of the pipe

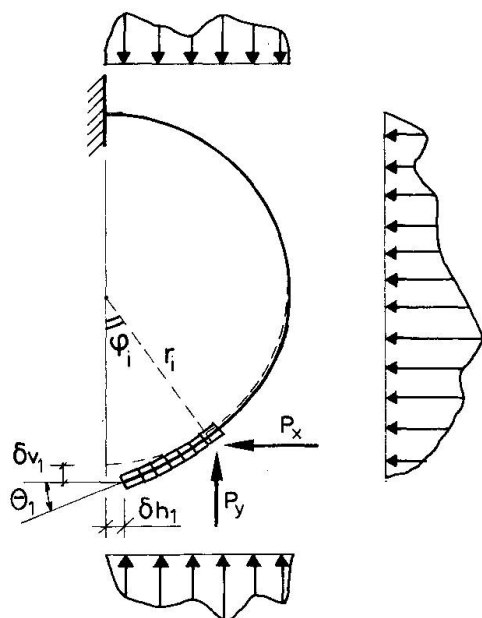
2α = bearing angle

To determine the earthload, the system stiffness λ (the ratio between stiffness of the pipe and the ground around the pipe) is very important. With a relative low value of λ , Q_v will increase by the deformation of the pipe.

Fig. 3 Schematization of the external loadings in the pipe

INTERNAL DISTRIBUTION OF THE LOADS

As the study is confined to the circumferential analyses of concrete pipes, longitudinal bending moments are not included. This is deemed to be a permissible simplification where the properties of the trench bottom are uniformly distributed.



The flexural stiffness of the pipe-wall varies along the circumference, which effects the internal distribution of the loads.

With the help of a computer the problem can easily be solved. Half a circle is divided in a number of segments of which the loads and the flexural stiffness are determined.

The pipe is assumed to be restrained at one side (figure 4). As a result of the loads exists a horizontal displacement δ_h , a vertical displacement δ_v , and an angular rotation ϕ_1 .

For reasons of symmetry, ϕ_1 as well as δ_h , is equal to zero. In the bottom of the pipe a normal force N_1 and a moment M_1 acts.

Fig. 4 Arc of circle restrained



N_1 and M_1 are determined from:

$$\left(\sum_{i=1}^{50} \frac{r_i}{EI_i} \Delta\phi_i \right) M_1 - \left\{ \sum_{i=1}^{50} \frac{r_i^2}{EI_i} (1 - \cos\phi_i) \Delta\phi_i \right\} N_1 + \theta_1 = 0$$

$$\left(-\sum_{i=1}^{50} \frac{r_i^2}{EI_i} (1 - \cos\phi_i) \Delta\phi_i \right) M_1 + \left\{ \sum_{i=1}^{50} \frac{r_i^3}{EI_i} (1 - \cos\phi_i)^2 \Delta\phi_i \right\} N_1 + \delta h_1 = 0$$

where:

- r_i = distance from centre to centre of segment i ;
- ϕ_i = angle, which together with r_i determines the location of segment i (bottom pipe $\phi = 0$; upper side $\phi = \pi$);
- EI_i = flexural stiffness of segment i .

If N_1 and M_1 are calculated, the normal forces, the shear forces and the moments of all segments can be determined.

NEW LIMIT STATE

From practice it is known that pipes are often rejected and replaced on other grounds than structural ones. By leakage i.e. the earth next to the pipe will flow into the pipe with the ground-water. By this the horizontal supporting pressure Q_h disappears and the pipe fails.

To determine the remaining lifetime of the pipe the usual assessment criteria are not suitable. A new criterion in terms of deflection of the pipe, seems obvious.

Deflection is the ratio between the vertical displacement of the pipe and the mean diameter of the pipe and can be expressed as percentage.

The advantage of this criterion is the fact that probably in the near future the connection between crack width and leakage will be found.

In the service limit state deflection, the pipe will be checked on its strength properties (sum of the moments, shear stresses and radial tensile stresses).

DESIGN MODEL

With the assessment criterion deflection both the loads and the internal distribution of the forces can be determined. The pipe may be cracked at maximum four places (the upperside, the bottom and two sides (figure 5)).

These cracks are assumed to be hinges. From the point of view of equilibrium a minimum sum of moments has to be resisted in these hinges. The pipe is assumed to collapse if these minimum sum of the moments cannot be resisted or if a fifth hinge exists.

The design model can be divided into two parts:

- a. Determination of the loads at the limit state deflection;
- b. Checking the strength of the pipes under these loads.

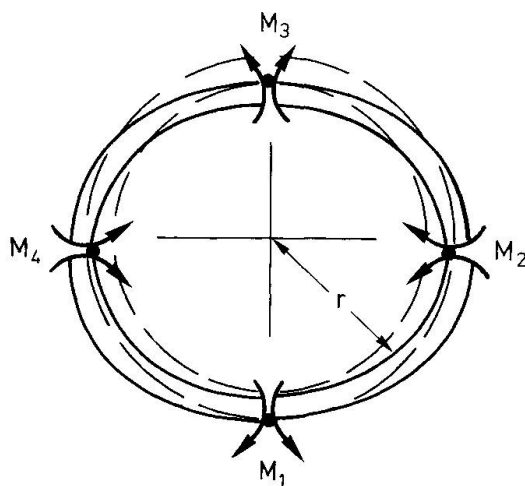


Fig. 5 Sum of the moments in a cracked pipe

- re a. Only the earth load, live load and surcharge are assumed to be depending on the deflection of the pipe. To determine these loads two different ways are possible:
- to adapt the flexural stiffness of the undamaged pipe till the assumed deflection is found;
 - to ascertain the loads directly at a fixed maximum deflection [1].
- re b. In the case of reinforced pipes the moment will be resisted by reinforcement, in the case of plain pipes by the eccentricity of the normal force. If the sum of the moments cannot be resisted the pipe is assumed to fail.
- Other checks in the model are: the possibility of the development of a fifth hinge and check of the shear forces and radial tensile stresses (see flow diagram figure 6).

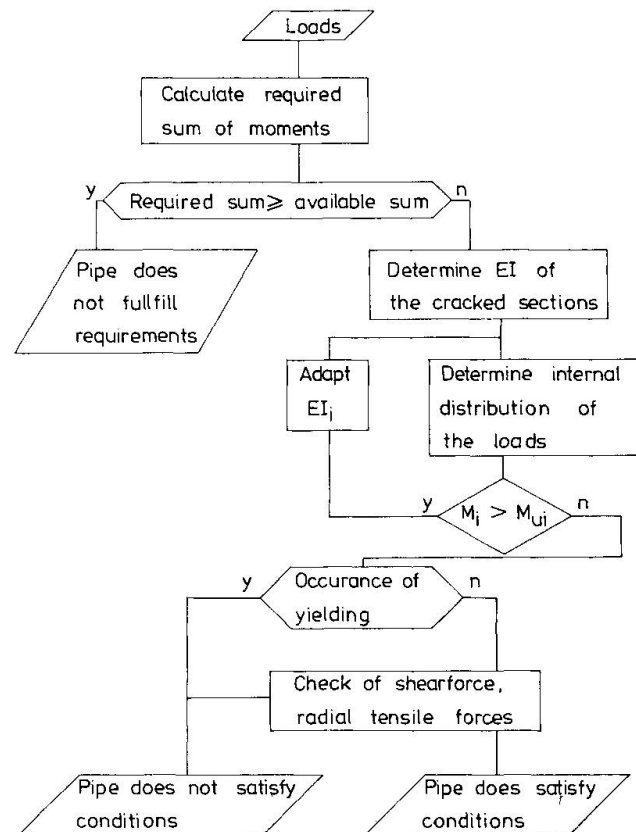


Fig. 6 Flow diagram design model

REMAINING LIFE EXPECTANCY

With the developed design model an indication of the remaining life-time of a concrete sewer pipe can be found; the exactness depends on the data concerning deterioration. Especially knowledge of the speed of the deterioration is important.

Figure 7 shows how this remaining life-time can be determined, assuming that the deterioration is linear in time and only the part above the water-level has been damaged.

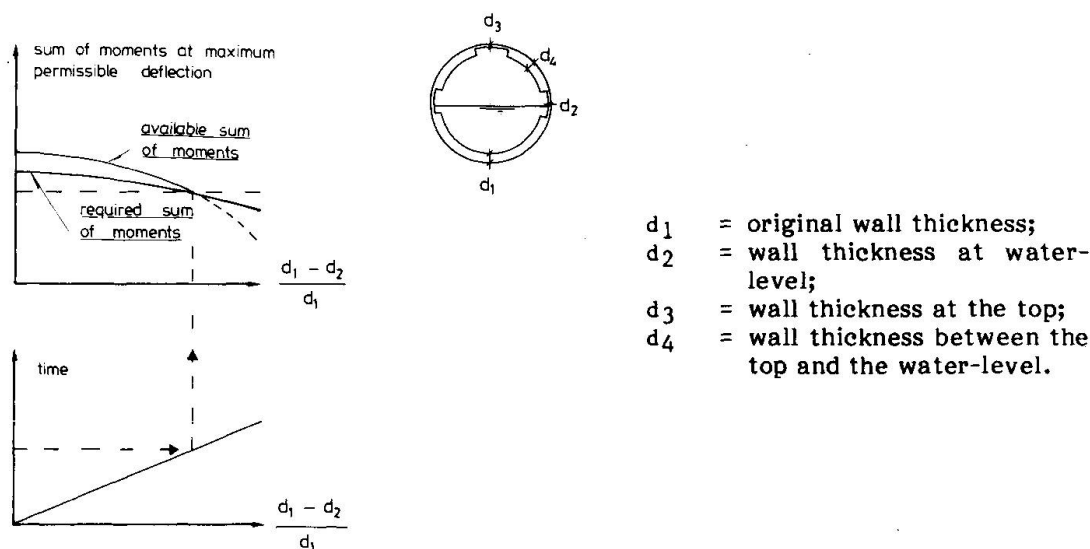


Fig. 7 Example of the determination of the remaining life-time

The speed of the deterioration at the water-level and at the top is two times the speed at the part in between.

The factor $\frac{d_1 - d_2}{d_1}$ gives the extend of the deterioration.

REFERENCES

1. EGAS, M., Opzet en uitwerking van een rekenmodel van aangetaste betonnen rioolbuizen. Delft University of Technology, Graduate thesis, 1988.
2. POLDER, R.B., Duurzaamheid rioolleidingen, een literatuurstudie naar aantastingsmechanismen. TNO-CHO-IBBC report 17, 's-Gravenhage, 1987.
3. POMEROY, The problem of hydrogen sulphide in sewers. 1976.
4. CUR-rapport 122, Buizen in de grond. CUR Gouda, 1986.

Application of Weathering Steel to Highway Bridges

Application aux ponts routes d'un acier résistant à l'action des intempéries

Verwendung witterungsbeständigen Stahles in Autobahnbrücken

Minoru FUJIWARA

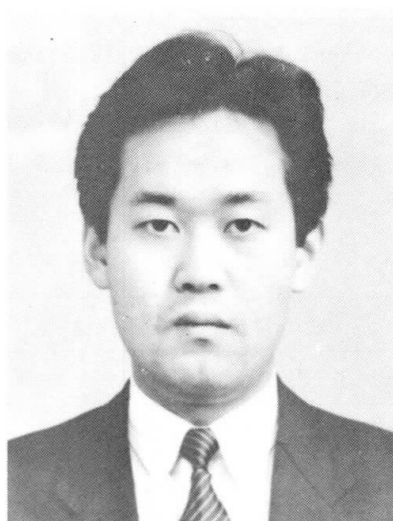
Head, Bridge Div.
Public Works Res. Ins.
Tsukuba, Japan



Minoru Fujiwara, born 1942, received M. Eng. at Nagoya University in 1967. He has been engaged in bridge engineering works and road administration at M.O.C. since 1967.

Jun MURAKOSHI

Res. Eng., Bridge Div.
Public Works Res. Ins.
Tsukuba, Japan



Jun Murakoshi, born 1963, received M. Eng. at Tokyo Institute of Technology in 1987. He has been engaged in bridge engineering works at M.O.C. since 1987.

SUMMARY

This paper outlines the present situation regarding utilization of weathering steel in Japan, the results of exposure tests, and the summary of "The Guideline for Design and Fabrication of Unpainted Weathering Steel Bridges (draft)" prepared by the Public Works Research Institute, the Ministry of Construction.

RÉSUMÉ

Cet exposé présente la situation actuelle de l'acier résistant à l'action des intempéries au Japon, les résultats des essais d'exposition ainsi qu'un résumé du projet de "Directives de conception et de fabrication des ponts en acier résistant à l'action des intempéries et non recouverts de peinture", préparé par l'Institut de Recherche des Travaux Publics et le Ministère de la Construction.

ZUSAMMENFASSUNG

Der Artikel gibt einen Überblick über den Stand der Verwendung witterungsbeständigen Stahles in Japan, die Ergebnisse von Verwitterungsversuchen, sowie über die vom Forschungsinstitut für öffentliche Bauten und dem Bauministerium herausgegebenen "Auslegungs- und Herstellungsrichtlinien für wetterfeste Brücken mit Anstrich (Entwurf)".



1. INTRODUCTION

Weathering steel has the property of preventing the further progress of rusting by the formation of a dense and stable rust layer on its surface.

The formation of such a dense and stable rust layer requires a certain environmental condition, such as no adhesion of salt and exposure to repeated drying and wetting, etc. Therefore, in application of weathering steel to highway bridges in rather severe condition of Japan, careful prior examination has to be required.

For this reason, Public Works Research Institute has started the study on application of weathering steel to highway bridges to clarify the suitable environmental conditions for weathering steel bridges and to establish their design and fabrication method. 10 year exposure test of plate specimens has been being carried out at 41 locations throughout the country in this study. The results of the exposure test for the first 3 years were used to prepare "The Guideline for Design and Fabrication of Unpainted Weathering Steel Bridges(draft)" in 1986.

This paper outlines the present situation of utilization of weathering steel in Japan, the results of the exposure test, and The Guideline of Design and Fabrication of Unpainted Weathering Steel Bridges(draft).

2. THE PRESENT SITUATION OF UTILIZATION OF WEATHERING STEEL IN JAPAN

Japan set JIS Standards of weathering steel in 1968, when weathering steel began to be utilized. The JIS Standards include W-type in which weathering steel is used with no treatment or it is used after rust stabilizing surface treatment, and P-type in which it is used after painted, as shown in Table 1.

Table 1 Chemical composition of weathering steel

		Chemical components (%)								
		C	Si	Mn	P	S	Cu	Cr	Ni	Others
SMA 50	W	≤0.18	0.15 } 0.65	≤1.40	≤0.035	≤0.035	0.30 } 0.50	0.45 } 0.75	0.05 } 0.30	Chemical elements effective for weather proofing such as Mo, Nb, Ti, V and Zr can be added to any type of weathering steel. However, the total of these elements should not be more than 0.15%.
	P	≤0.18	≤0.55	≤1.40	≤0.035	≤0.035	0.20 } 0.35	0.30 } 0.55	—	

P-type weathering steel with painting treatment is hardly applied to bridges now because the effect of paint for weathering steel bridges is not sure in comparison with ordinary painted steel bridges.

The rust stabilizing surface treatment is a method to promote the formation of a stable rust layer by covering the surface of W-type weathering steel with porous

film, and the film disappears after the formation of the stable rust layer. This method has been applied to bridges, as means to control the stable rust layer and to improve the appearance at the early stages of the formation of the stable rust layer. However, it seems the effect of this method are not clear.

When the poor appearance in the initial stage is allowed and good care is taken to prevent the contamination of the surroundings by the rust film, the use with no treatment is advantageous in terms of the initial cost and the maintenance cost. In the future the use with no treatment is likely to become the main method. The Guideline(draft) mentioned above is also for W-type steel to be used with no treatment.

As shown in Fig.1, the consumption of unpainted weathering steel has increased gradually, and the recent annual consumption reaches approximately 10,000 tons in steel weight or 60 cases yearly.

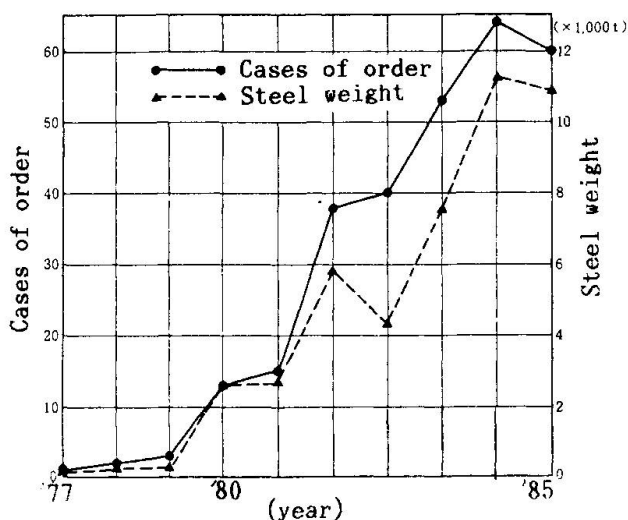


Fig.1 Trend in application of unpainted weathering steel to bridges

3. NATIONWIDE EXPOSURE TESTS OF PLATE SPECIMENS

3.1 Outline of the Tests

3.1.1 Test Specimens

The size of test specimen is 100mm×150mm×8mm, and both the surface and the back are subjected to blasting treatment. The chemical composition of the test specimen meets the JIS Standards.

3.1.2 Environmental Condition at Exposure Locations

The test specimens are placed on actual bridges at 41 locations in different environmental conditions (coastal area, mountainous area, rural area, urban area, and industrial area) extending from Hokkaido to Okinawa. The amount of the airborne salt(NaCl) and the amount of SO₂ were measured for 1 year at the exposure locations in order to examine the relations between these factors and the quantity of corroded weathering steel.

3.1.3 Placement of Test Specimens

The test specimens are placed at lateral bracing in the horizontal and vertical directions, where the corrosive condition is most severe in actual bridges.

3.2 Results of the Tests

3.2.1 Annual Change in Corroded Steel

Typical examples of the results, which were obtained by converting the results of weight analysis of test specimens to the reduction in the plate thickness of one



side of the test specimens are given in Fig.2(a) and (b). Fig.2(a) refers to the annual change in the plate thickness reduction of test specimens exposed in areas along the Pacific coast. The rate of plate thickness reduction proceeds rather quickly. This indicates that the environmental condition of the locations does not allow the use of unpainted weathering steel. Fig.2(b) illustrates the plate thickness reduction of test specimens exposed in the inland rural area. The case of (b) shows less plate thickness reduction in comparison with the case of (a).

Weathering steel can perform its original function by the formation of a stable rust layer. It takes a fairly long time before one can identify the stabilization of rust from testing. In good environmental condition as shown in Fig.2(b), it is assumed that it takes a much longer time before the formation of a stable rust layer, because rusting itself proceeds very slowly.

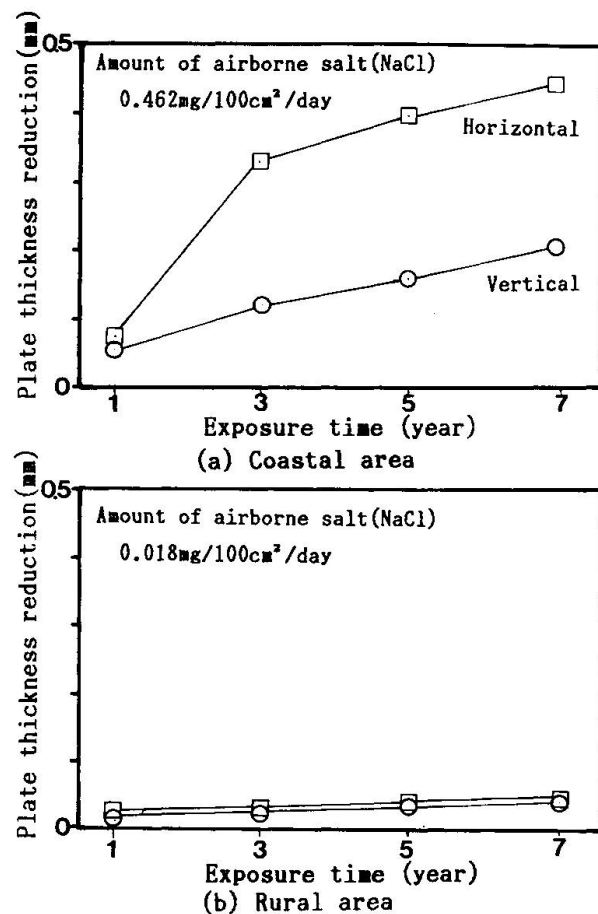


Fig.2 Annual change in plate thickness reduction

3.2.2 Relations between Environmental Conditions and the Quantity of Corroded Weathering Steel

The results of the 3 year exposure test indicate that the plate thickness reduction in 50 years assumed by data extrapolation is less than 0.4 mm at 17 locations in mountainous, rural and urban areas, while the total plate thickness reduction after 3 year exposure is more than 0.2 mm, or the unstable stratified rust is formed on the steel surfaces at 10 locations in Okinawa, the Sea of Japan coastal areas and the areas facing the open sea. Fig.3 summarizes the results of the exposure tests at 41 locations all over the country; the former areas are marked with a white circle. The latter areas are marked with a black circle. Other unclassified areas which do not belong to either of them are marked with a black dot.

Broadly speaking, the following can be conducted as to environmental conditions: The environmental condition in Okinawa, the Sea of Japan coastal areas and the Pacific coast areas facing the open sea is generally unsuitable for weathering steel bridges. In particular, in the Sea of Japan coastal areas, the areas placed fairly distant from the coast even in a plain, if it opens in the seasonal wind direction, are unsuitable. In contrast, in mountainous areas excluding Okinawa, and plains excluding the above, many of them are suitable. Further observation of

the future exposure tests results is necessary for judgement at the locations which are close to relatively calm sea such as Setouchi Inland Sea.

Fig.4(a) and (b) show the relations between the amount of NaCl, and the amount of SO₂ and the plate thickness reduction after 7 year exposure. The classification of the marks used in these figures is same as those used above. These figures indicate the plate thickness reduction correlates much with the existence of airborne salt and less with the existence of SO₂ in their environment.

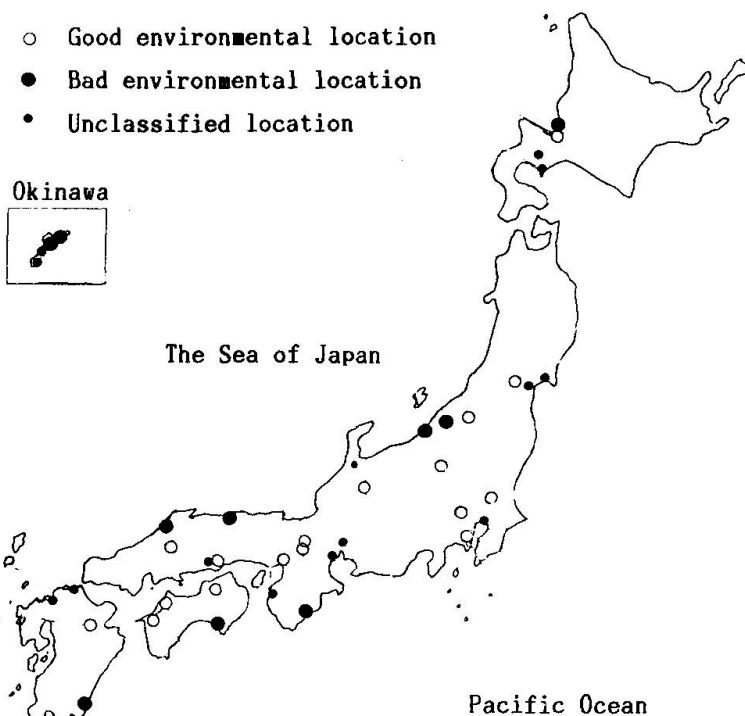


Fig.3 The results after 3 year exposure

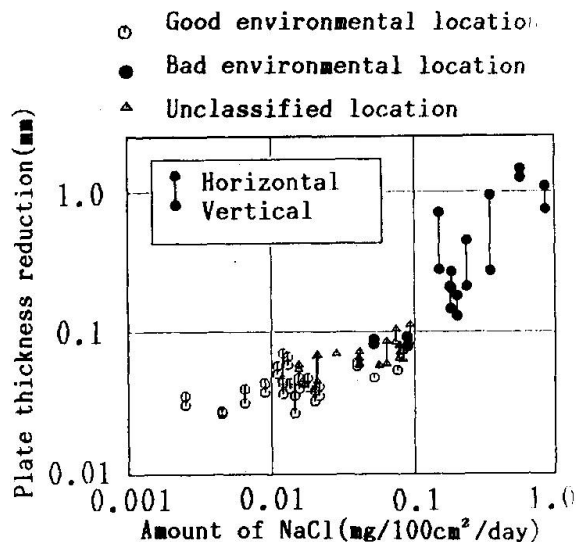


Fig.4(a) The relation between the plate thickness reduction after 7 years exposure and the amount of NaCl

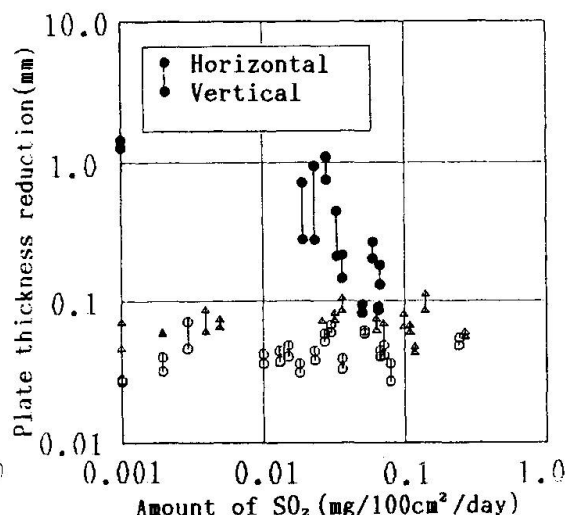
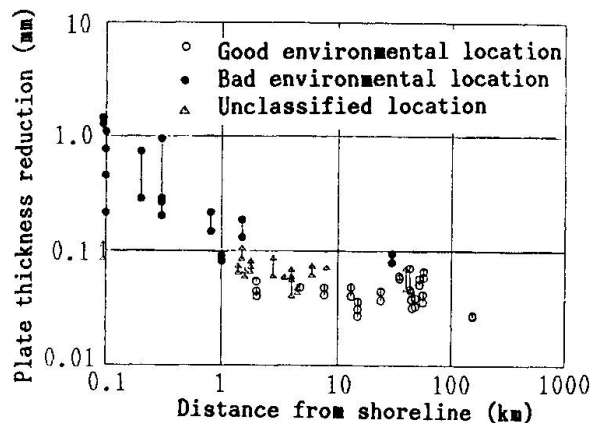


Fig.4(b) The relation between the plate thickness reduction after 7 years exposure and the amount of SO₂



Besides, Fig. 5 shows the relation between the linear distance of exposure locations from the shoreline and the plate thickness reduction. This figure suggests that the plate thickness reduction correlates with the distance from the shoreline.



4. THE GUIDELINE FOR DESIGN AND FABRICATION OF UNPAINTED WEATHERING STEEL BRIDGES (DRAFT)

The Guideline (draft) was prepared in 1986 based on the results of the 3

year exposure tests as reference information for application of unpainted weathering steel to bridges. The Guideline (draft) is a kind of interim report in the 10 years program. In the Guideline (draft), area of country was divided into following 3 categories;

- 1) Area where the effect of airborne salt is minor and unpainted weathering steel can be used
 - a) Mountainous areas
 - b) Rural areas and Urban areas (but coastal areas and plains opening towards the sea are excluded)
- 2) Areas where unpainted weathering steel can not be used because of serious effect of airborne salt.
 - a) All of Okinawa
 - b) Japan Sea coast areas and other areas facing the sea directly

The basic ideas for dividing areas is given below: The plate thickness reduction in 50 years at 41 locations is assumed by extending the linear line intersecting the plate thickness reduction in 1 year and that in 3 year. Taking account of the fact that the rate of the plate thickness reduction gets smaller with the lapse of time, this assumed value gives a figure on the safe side. When the plate thickness reduction after 50 years is equal or less than that due to the formation of a stable rust layer, then there is no serious problem even if the rust is not yet stabilized. It has been recognized that the formation of a stable rust layer results in the plate thickness of approximately 0.1~0.2mm even in an good environmental condition. In the Guideline (draft), the limit was set as 0.4mm in consideration of the measuring precision of the plate thickness reduction, and suitable areas is thus judged. On the other hand, when the plate thickness reduction after 3 year exposure exceeds that (0.2mm) due to stable rust, or unstable stratified rust can be seen by the serious effect of airborne salt, we can not expect the formation of a stable rust layer, and non-suitable areas are thus judged.

The guideline (draft) also mentions the notice on design and fabrication of unpainted weathering steel bridges.

Fig. 5 The relation between the distance from the shoreline and the plate thickness reduction after 7 years exposure

Road Subway under the Railway Line in Mestre
Passage souterrain sous la ligne ferroviaire à Mestre
Unterführung der Eisenbahnlinie in Mestre

Salvatore VENTO
Head
Roads and Traffic Dep.
Mestre-Venice, Italy



Salvatore Vento born 1948, graduated in Engineering at Padova University in 1973, has been working for the technical department of the Venice local authority.

Massimo BOTTACIN
Civil Engineer
Mestre-Venice, Italy



Massimo Bottacin was born in 1950. He graduated in Architecture at Venice University (1973) and in Engineering at Bologna University (1979). After working in the technical Dep. of the Furlanis Group of Contracting Companies, he is now a free-lance consultant.

SUMMARY

This paper describes a prefabricated road subway for the Venice-Trieste railway line, constructed using a technology whereby it was "driven into place" to avoid interrupting the railway traffic, and overcoming waterproofing problems due to the existence of the groundwater.

RÉSUMÉ

L'article décrit le passage souterrain préfabriqué de la ligne ferroviaire Venise-Trieste réalisée à partir de la technologie de mise en place "par poussée" afin d'éviter l'interruption du trafic sur les voies, et de surmonter les problèmes d'impérméabilisation liés à la présence de nappes phréatiques.

ZUSAMMENFASSUNG

Der Artikel beschreibt die vorgefertigte Unterführung der Eisenbahnlinie Venedig-Triest, die ohne Unterbrechung des Bahnverkehrs mit der "Schub"-Technologie verwirklicht wurde, und zwar im Grundwasser mit den dadurch bedingten Abdichtungsproblemen zur Erreichung eines dauerhaften Bauwerks.



1. INTRODUCTION

The road tunnel under the via Terraglio, at km No. 2 - 773 of the Venice-Trieste railway line, comes within the scope of a much larger project for eliminating the level crossings in the renovation and improvement of the Mestre road communications network.

The choice of the subway solution was dictated by technical considerations as well as concern for the environment and the appearance of the structure: an overpass would have proved difficult to connect to the existing ground-level road network, though the nature of the soil and existence of a water bed very close to the surface involved difficulties in the subway project's execution and extra problems of maintenance and durability.

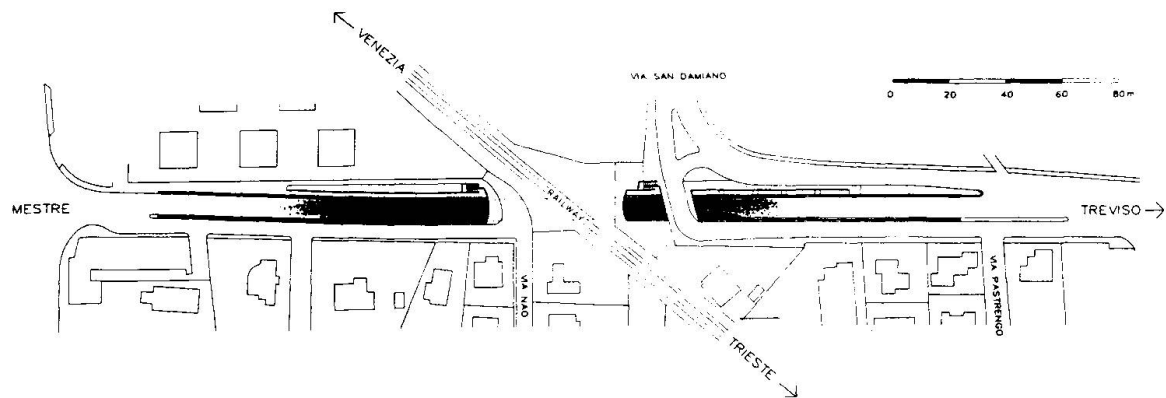


Fig. 1 - General planimetry

The subway comprises an underground section 47.50 m long under the railway tracks with open-air ramps on either side for a total overall length of about 300 m with maximum longitudinal gradients of 1 in 12.5.

The road carriageway is 7.50 m wide with side lanes and has a minimum height of 5.00 m inside the tunnel: there is a footpath running parallel to the road, with the same gradients but raised with respect to the road surface both for safety reasons and to enable the passage under the railway of the technological utilities contained in an underlying trench duct, the footpath is also linked to the ground level by flights of steps just outside each end of the tunnel (fig. 8).

2. NATURE OF THE LAND

The stratigraphic nature of the land may be summarized as follows: beneath a couple of meters of top soil, there is a poorly-compacted layer of sand and silt with a lenticular trend; from 4 to 10 meters in depth, there is sand and salty silt alternating in thin moderately-consistent cohesive strata, from 10 to 24 meters, there is a moderately-compacted sand and silt layer, generally involved with a thin clay and silt stratum, followed by clayish silt and slimy sand. The depth of the water bed is about 1.50 m underground.

3. TECHNICAL SOLUTION USED AND PROJECT STAGES

The technique adopted for passing the existing important railway line without

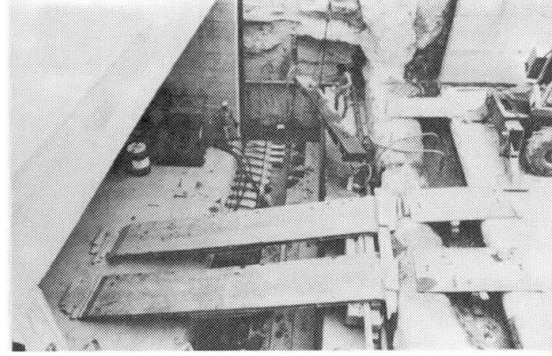
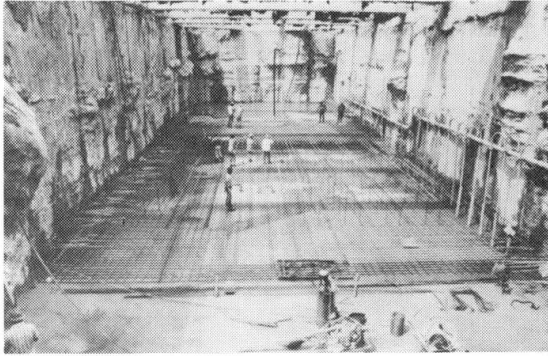


Fig. 2 - Construction of launching bed

Fig. 3 - Hydraulic jacks

interrupting normal railway traffic is based on the construction of a pre-fabricated reinforced concrete element (monolith) and its subsequent pushing into place under the railway line by means of hydraulic jacks.

The project stages included the initial construction of continuous walls of reinforced concrete diaphragm plates cast in the presence of bentonite mud, partly strutted against each other at the tops and partly left free, with a maximum length of 24 m sunk to a depth sufficient to counter water infiltration and arranged with a closed-perimeter tank layout to allow for excavations inside them for the construction of the concrete monolith and ramps for access to the subway.

This method was chosen because of the geotechnical features of the soil and more particularly because of the subway's location in the vicinity of buildings and the existence of the water bed very close to the surface for

which artificial lowering was unacceptable. A reinforced concrete floor slab 1.0 m thick (fig. 2) was then cast in the first tank, near the railway bed, at a depth of 9.60 m from the plane of site, to provide the support for the construction of the monolith and the surface for sliding and guiding said monolith; it was completed with a thrust-bearing wall for countering the jacks during shifting operations.

The monolith was then constructed, forming a boxed structure made of reinforced concrete with an overall size of 12.60 m wide by 7.60 m high by 43.50 m long and a constant thickness of 1.05 m; the driving side sloped away at a 45 angle and its perimeter was shaped for sharpness.

In the next stage, after demolition of the diaphragm wall standing in

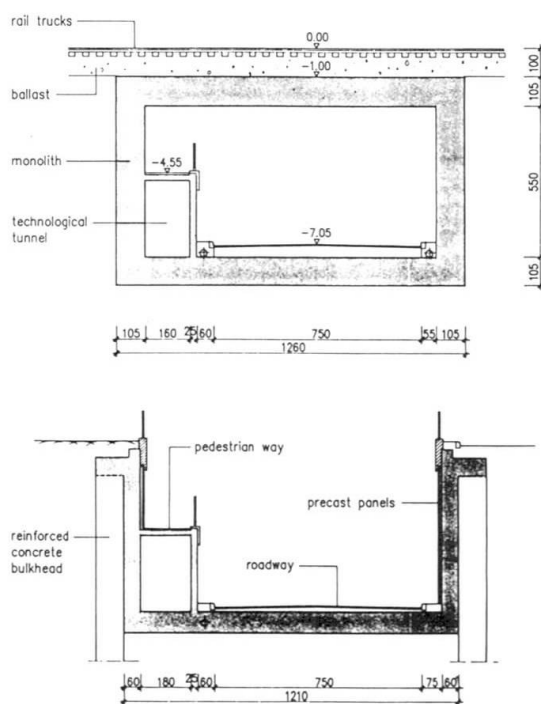


Fig. 4 - Sections

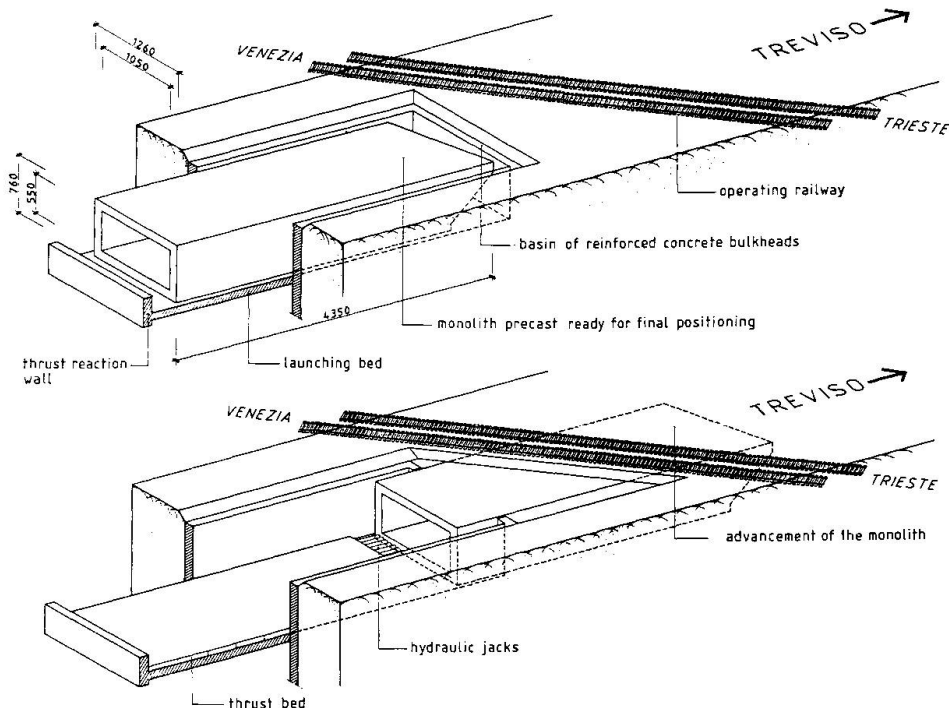


Fig. 5 - Scheme of the positioning operations

front of the railway line, this monolith (weighing about 4.000 metric tons in all) was driven into place by 30 hydraulic jacks, divided into three groups and operating simultaneously but independently in order to correct any rotation of the structure (fig. 3).

A number of coupled IPE 600 metal girders, arranged under the sleepers so that they rested on a layer of sliding rollers on the top slab of the monolith and on the ground on the other side, enabled the tracks to be supported during the monolith-driving operations without interrupting railway traffic.

In the area under the tracks, hydraulic protection of the advancing face during the shifting stage was provided by two continuous longitudinal walls of high-pressure jet-grouted concrete piles 16 m long, placed side-by-side.

After the monolith had been driven into place, the access ramps were constructed of "U"-shaped structures composed of slabs and walls cast against diaphragm plates.

Sealing of the casting joints between the wall and the slab was done by inserting an expanding water-stop beading made with sodium bentonite and butyl rubber.

The risk of floating due to hydrostatic pressure from below was overcome by connecting the walls of the "U"-shaped structures with the tops of the reinforced concrete diaphragm plates, thus increasing the load brought to bear. The faces of the ramp walls were lined with self-supporting reinforced concrete square-corrugated panels, placed in such a way as to leave a cavity of a few centimeters to enable air circulation and the collection of any infiltrated water in the bottom for channelling into the main drainage system.

4. RAINWATER POUR-OFF SYSTEM

The rainwater pouring down the road and footpath ramps is intercepted by several crosswise grid-covered ducts and, together with any infiltrated water, is poured off by pipelines embedded in the concrete slabs to two pumping units situated at the foot of the ramps on each side of the subway.

The overall flow rated for the maximum intensity of rainfall has been calculated at 117 lt/sec and each of the pumping units has been fitted with two electric pumps for a delivery of 60 lt/sec each and for a head of 13 m as the water has to be raised to the level of the town's sewage system. In the case of breakdown of either pumping unit, the two pumps in the other unit are sufficient to raise the full flow of water: to cater for this possibility, the pits housing the two units are connected by a pipeline under the road through the subway.

Each pump has an absorption of 11.2 KW and is supplied normally from the mains electricity but also has a stand-by generator on ground level for emergency use.

5. STEPS TAKEN TO ENSURE DURABILITY FOR THE MONOLITH

As the structure is entirely underground and in the presence of water, durability had to be ensured with regard to the environmental conditions (which are moderately aggressive), to the kind of forces coming to bear and to the type of reinforcement (which is not very susceptible to corrosion) so a test calculation for the structure's cross-section was done in cracking limit conditions according to the CEB FIP model code using a nominal value of $W_2 = 0.2$ mm.

After calculating the mean opening of the cracks (W_m) for the mean yield (ϵ_{sm}) generated on the mean distance between cracks (S_{rm}), it was decided that the value specified by the characteristic value $W_k = 1.7 \times W_m$ was not to be exceeded.

The reinforcement was arranged in two layers with a concrete cover of 4.5 and 10 cm respectively, using class Rbk = 30 MPa concrete on the assumption of a resistance to simple tensile stress of $f_{ctm} = 2.6$ MPa.

To reduce cracking due to hydraulic shrinkage, the concrete was made using the combination of a superfluidifying additive with an expanding agent.

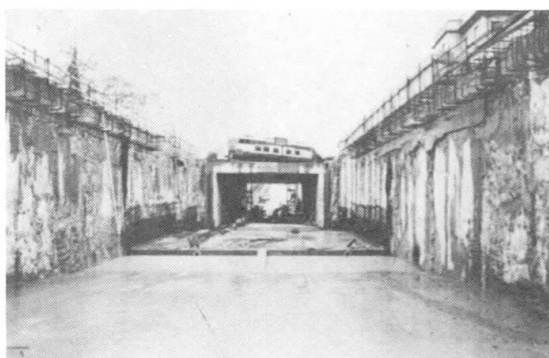


Fig. 6 - Launched monolith

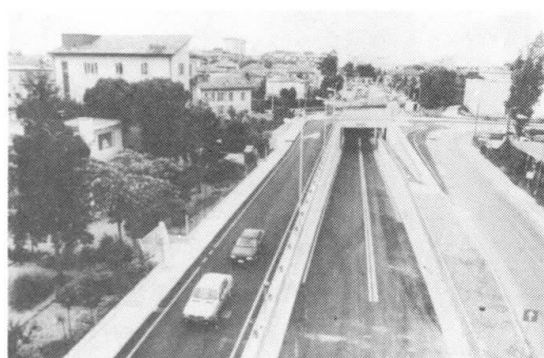


Fig. 7 - View of the completed subway



The superfluidifying additive not only gave the mix the necessary workability (22 cm slump), resulting in a concrete with a lower permeability (due to lowering of the water/cement ratio) and a higher initial mechanical compressive strength, it also enabled a controlled-shrinkage concrete to be produced with smaller quantities of expanding agent.

The mean shrinkage of the concrete in place after 6 months was calculated in $380 \mu / m$ and the expansive agent was proportioned on this value.

The castings were cured by keeping the concrete wet and protected from evaporation with tarpauline for four days, though the expanding process was over in one day.

About one month after completion of the castings, the walls of the monolith were waterproofed by brush-application of an impregnating solvent-based primer on the outside; as the roofing slab was susceptible to greater mechanical stress during shifting of the monolith because of the sliding of the metal girders supporting the railway tracks, this was waterproofed with a two-component epoxy resin, which was touched up in any damaged areas after the monolith was in place.

The bottom slab was treated on the inside with elastomerized bitumen before laying the road surface.

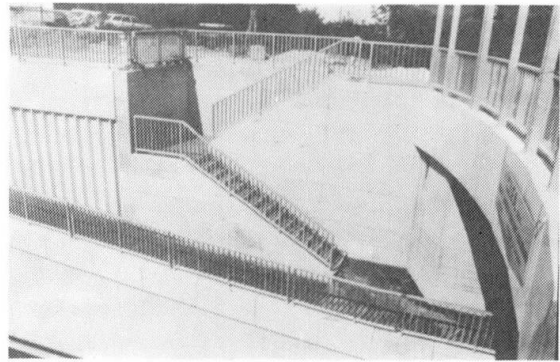


Fig. 8 - View of a flight of steps

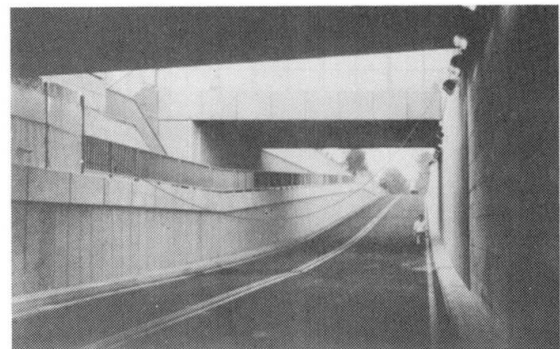


Fig. 9 - View of a ramp

6. MONOLITH CONCRETE COMPOSITION AND FEATURES

- Slump : 22 cm
- Cement : 325 Portland - 340 kg
- Dry aggregate max diameter 25-27 mm - 1900 kg
- Water : 170 lt
- Water/Cement ratio : 0.50
- Aggregate/Cement ratio : 5.60
- Compressive strength after 1 day : $R_{mb} = 9 \text{ MPa}$
- Compressive strength after 28 days : $R_{mb} = 36 \text{ MPa}$
- Shrinkage after 6 months : $380 \mu / m$
- Naphthalene sulphonate polymer superfluidifier (NSP) : 3.4 lt
- Expanding agent with special clinker rich in free lime : 25 kg

7. ACKNOWLEDGEMENTS

The authors's thanks go to the CIFA s.p.a. Contracting Company of the Furlanis Group for their precious contribution in the performance of the work.

Durability of Precast Concrete Underground Containers

Durabilité de réservoirs souterrains préfabriqués en béton armé

Dauerhaftigkeit vorgefertigter erdversenkter Behälter

P. H. CHUANG

Lecturer

Nanyang Technological Institute
Singapore



Dr. Chuang received her PhD in Civil Engineering from Imperial College, London. Before that, she worked in a consulting firm, involved in design and supervision of various concrete and steel structures. She is now a lecturer in the area of structures and construction.

J. ALUM

Professor

Nanyang Technological Institute
Singapore



Dr. Alum received his Dr. -Ing. degree from the Technical University of Karlsruhe in 1964. He worked in various civil engineering projects in Bangladesh, United Kingdom and North Africa. In 1982, he joined Nanyang Technological Institute as Associate Professor. He is a member of the Institution of Civil Engineers, London.

SUMMARY

This paper describes a segmental construction method for small waterproof reinforced concrete underground containers. Special aspects involving durability of such structures are discussed and highlighted.

RÉSUMÉ

L'article décrit une méthode de préfabrication de réservoirs souterrains en béton armé imperméable. Des aspects spéciaux quant à la durabilité de ces structures sont exposés.

ZUSAMMENFASSUNG

Die vorliegende Veröffentlichung berichtet über ein Konstruktionsverfahren für kleinere, erdversenkte, wasserdichte Stahlbetonbehälter. Besondere Aspekte der Dauerhaftigkeit derartiger Bauten werden besprochen.



1. INTRODUCTION

Waterproof reinforced concrete underground containers are usually constructed by supporting the sides of excavation and concreting the container structure in-situ. For small container structures built to a depth of, say 6 metres, the cost of supporting the soil can be high, which may in certain cases be equal to the cost of the structure itself. Alternatively, if the site conditions allow, sheet piling or other forms of soil supports can be conveniently avoided by using open cut with appropriate side slopes. Nevertheless, this may fall foul of the safety regulations[1] and under heavy rains and wet conditions can lead to slope failure, causing hazard to human lives[2].

A precast cum cast-in-place method was developed to construct an underground container (14.4 m long x 3.7 m x 3.85 m deep) in an open cut in stiff clay[3]. The second year civil engineering students of Nanyang Technological Institute completed the construction of the container in an eight-week period. The work was carried out in two phases. In the first phase, 2.35 m deep precast segments with waterbars fixed to appropriate edges, were placed in the open cut at certain spacings (Fig. 1). These spacings were later filled with cast-in-place concrete. These precast units, in fact sheltered the "student workers" against any probable soil failure during very wet conditions. In the second phase, the structure was completed by finishing the upper 1.5 m of the structure with cast-in-place concrete.

This method of construction, created considerable amount of horizontal and vertical joints. These joints, unless properly detailed and constructed, may, during the service life of the container, lead to overall deterioration of the structure.

In this paper, details of the joints, selection of materials, quality control during construction and future monitoring of the performance of the joints are highlighted and discussed.

2. DETERIORATION OF UNDERGROUND CONCRETE CONTAINERS

Concrete is extensively used in the construction of underground containers. The subsoil and ground water environment can cause substantial damages to these structures during their service life due to interaction of aggressive elements like chlorides, sulphates and acids[4,5]. In such adverse exposure conditions, successful performance of underground structures depends mainly on their durability rather than on strength. Aggressivity of underground environment depends on the concentration of detrimental substances. Main characteristics of corrosive subsoils are low carbonic acid content, high degree of acidity, good conductivity and high salt and moisture content.

2.1 Deterioration of Cement Matrix

In concrete structures which remains permanently below ground water table, the deterioration processes are predominantly of the chemical type. For structures partially submerged, in the zone where groundwater level fluctuates, the chemical actions are augmented by alternate cycles of drying and wetting and other physical agents. Fluctuating ground water table can dissolve the calcium or magnesium sulphates that may be present in the subsoil and deposit them along the concrete surfaces. The sulphate action along with acid and microbial attack brings about a gradual concrete deterioration.

2.2 Deterioration of Reinforcing Steel

If the underground structure is exposed to saline groundwater conditions, the cement matrix is not much harmed, but the reinforcing steel can rust drastically. Rust causes large internal expansive forces which are sufficient to crack and eventually spall off the concret over the reinforcement. This type of damage, if allowed to proceed unchecked, can raise serious questions concerning performance, safety and reliability of the structure. If a decision is taken to repair the damage, the cost could be as high as 10% of the actual cost of the structure.

2.2.1 Corrosion of Reinforcing Steel at Joints

Joints of underground containers can be identified as causing great hazards to the reinforcement. If the joints open up at any time during the service life of the structure, mere penetration of moisture or water can contribute to the corrosion process of the reinforcing steel. This situation can also impair the water tightness of the structure and the structure may be considered as damaged and measures should be taken leading to repairs.

3. CONSTRUCTION OF A PRECAST CONCRETE UNDERGROUND CONTAINER

As mentioned earlier, an underground container was constructed on the Nanyang Technological Institute campus. It is intended to be used for the purpose of geotechnical testing. This container is meant to be waterproof.

In the first phase, 2.35 m high precast segments with waterbars fixed to appropriate edges, were placed on a prepared bed on the open cut at certain spacings (Fig. 2). The precast units in fact sheltered the "student workers" against any soil failure during wet condition. The spaces between the precast units were later filled with cast-in-place concrete. In the second phase, the structure was completed with cast-in-place concrete. The sequence of construction is illustrated in Fig. 1. Two types of precast elements, namely the end units and the internal units, were used. The precast units were cast on a yard near the open cut. A 90-ton capacity crane was used for handling and placing these units. After the completion of the first phase of concreting, the structure was backfilled by granular soil up to 300 mm below the top of this partly constructed container. This facilitated fixing of formwork for the second phase cast-in-place concreting of the rest of the container.

4. JOINTS AND THEIR TREATMENT

Laboratory tests confirmed that the soil surrounding the container are free from sulphates and other aggressive elements. As such, the main concern related to durability as well as watertightness of the container, was treatment of the joints. The reinforcement has to be adequately protected at the joints, because any easy passage of water through these joints, in course of the service life of the container, would cause severe rusting of the reinforcement leading to damage of the structure. Water bars were fixed at all joints of precast elements facing cast-in-place concrete (Figs. 2 & 3). The mix design was carefully specified with the emphasis being on a suitable water-cement ratio, optimum cement content along with workability consideration[6]; hence, during compaction, the water bars were reasonably secured at their positions. To provide further lines of defence against ground water penetration into the



container, bituminous coating underlying a polymeric membrane was placed all over the external surface of the container. All bolt holes were plugged with non-shrink cementitious material.

5. MONITORING PERFORMANCE OF THE UNDERGROND CONTAINER

As the container, under service conditions, will be subjected to a surcharge of 20 kN per sq m and various other loads, there is a possibility of differential settlements leading to joint movement. Any deterioration of the joints will be visually monitored and investigated.

6. CONCLUSION

Durability is one of the main criteria in the construction of underground concrete structures. The precast cum cast-in-place method, wherever applicable, is safer, faster and more economical than the conventional cast-in-place method. Also, the problem of deterioration of precast joints does not exist. However, the horizontal and vertical joints can cause durability problems for the structure. Suitably placed water bars at the joints, enhanced by a properly applied bituminous coating underlying a polymeric membrane will definitely help to achieve a satisfactory long term performance of the underground concrete container.

7. ACKNOWLEDGEMENTS

The successful application of the construction method mentioned in this presentation was achieved through the combined efforts of the Dean, the staff and students of the school of Civil and Structural Engineering of the Nanyang Technological Institute. The authors are very grateful to the School and Institute for the opportunity to participate in such a special exercise. A special thank is due to Mr David Chew for the figure used in this presentation.

REFERENCES

1. Republic of Singapore, Government Gazette, 1985.
2. The Institution of Structural Engineers, Proceeding of the Symposium on Design and Construction of Deep Basements, Ed: R.J.R. HANCOCK, May, 1981.
3. Nanyang Technological Institute, Information Manual for Students and Project Document, for the construction of a CSE Experiment Station - a sheltered trench for geotechnical testing. In House Practical Training Programme, School of Civil and Structural Engineering, March, 1988.
4. DORAN, S.R., ROBERY, P, ONG, H and ROBINSON, S.A. Corrosion Protection To Buried Structures. Proc. MRT Conference, Singapore, April 1987, pp. 215-224.
5. HARRISON, W.H., Durability of Concrete Structures in Acidic Soils and Waters. Journal of the Concrete Society, London, February 1987, pp. 18-24.
6. BRITISH STANDARD BS 8110: Structural use of concrete, Part 1 - Code of practice for design and construction, 1985.

SEQUENCE OF CONSTRUCTION FOR THE TRENCH

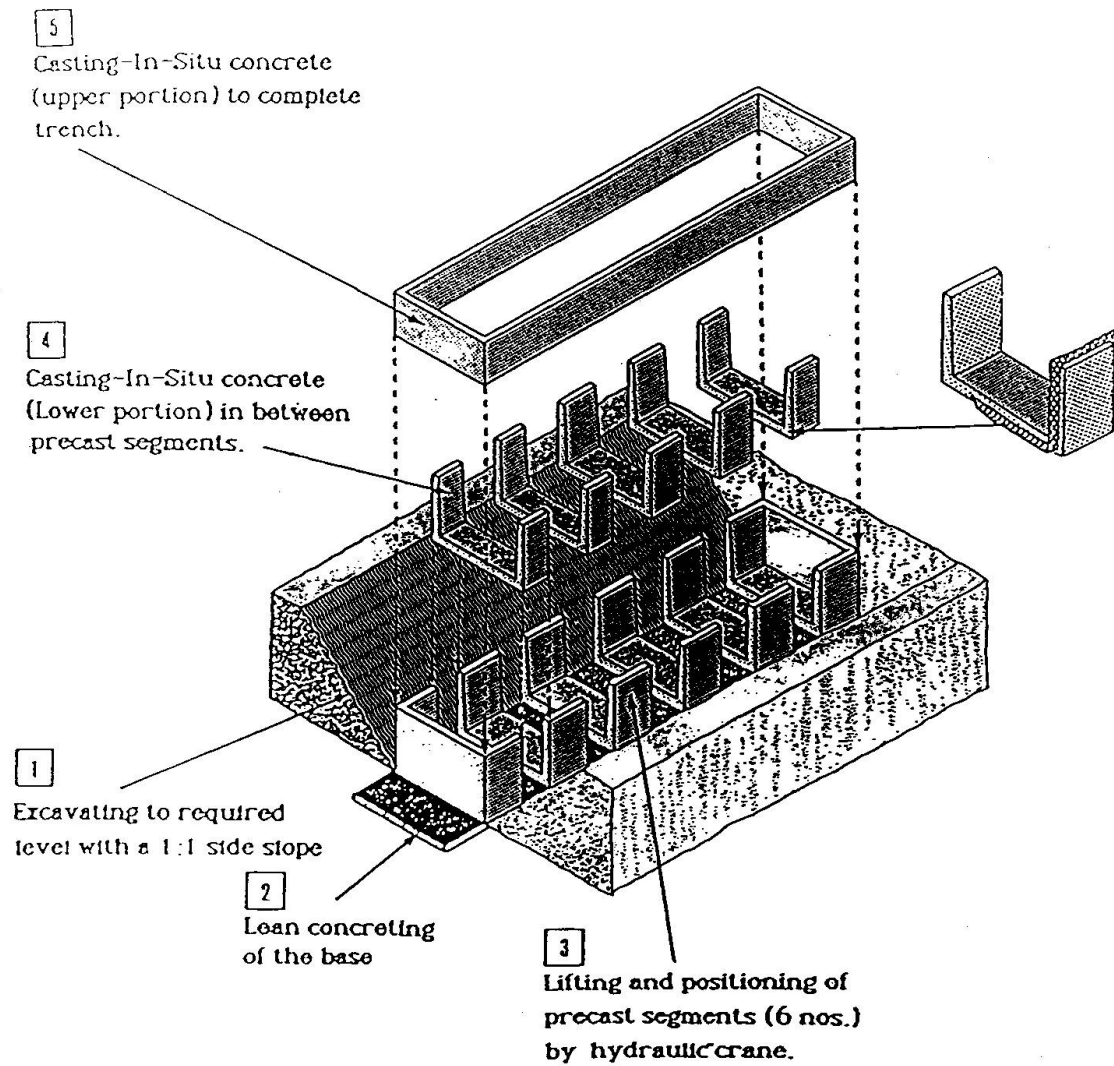


Fig.1 Sequence of construction

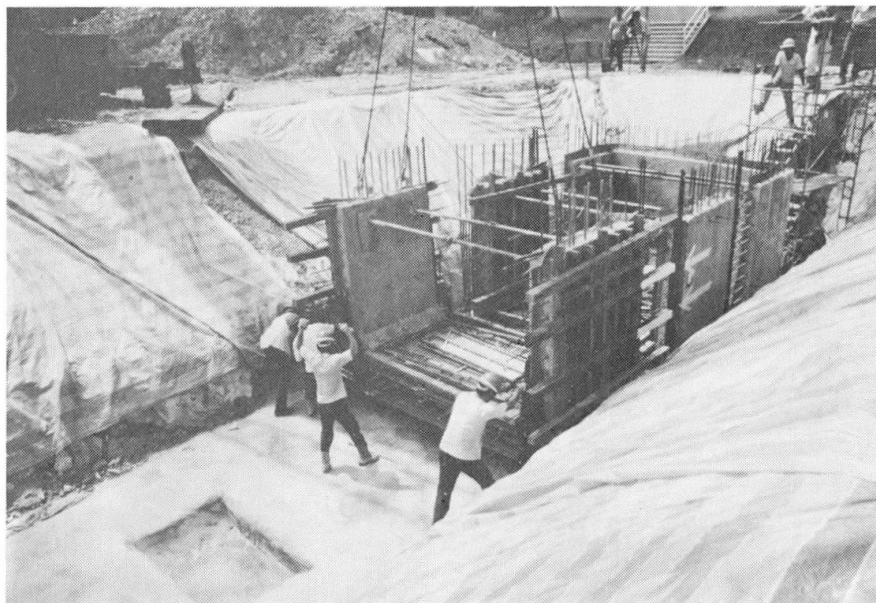


Fig. 2 Precast segments being placed on a prepared bed on the open cut at certain spacing,

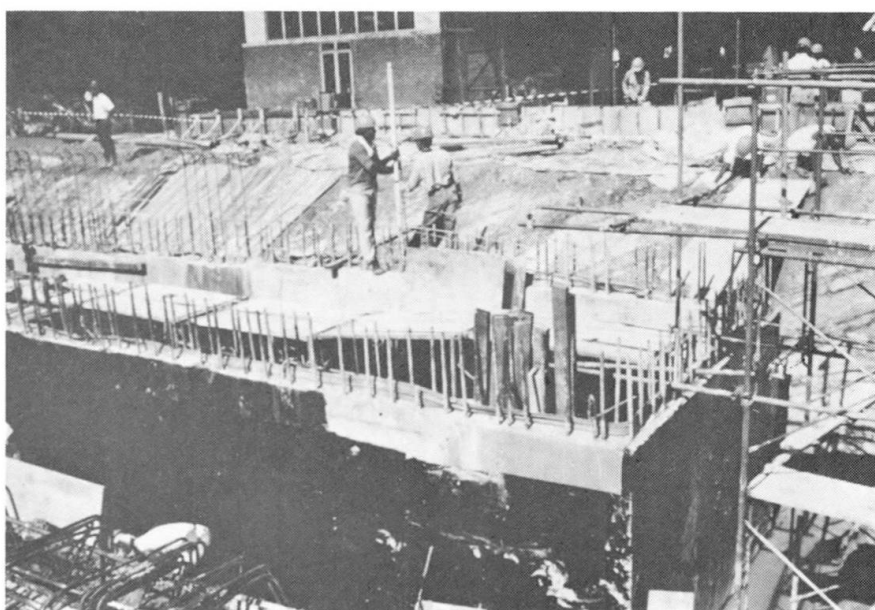


Fig. 3 End of Phase I.
Water bars have been fixed at joints facing Phase II
cast-in-place concrete.

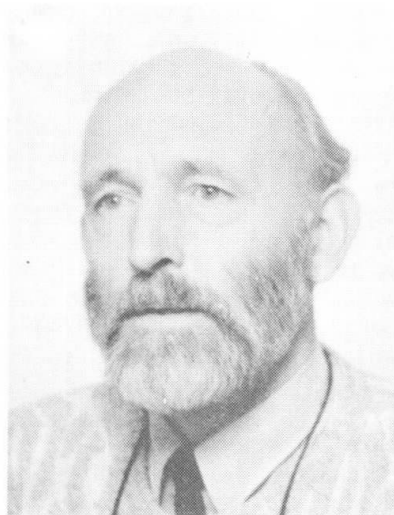
A New Housing Concept

Nouvelle conception pour la production des maisons

Ein neues Konzept zur Wohnungsproduktion

J. O. BATS

Assist. Professor
Eindhoven Univ. of Technology
Eindhoven, The Netherlands



Ir. J. O. Bats, born 1933, received his civil engineering degree at Delft University of Technology in 1964. He worked for several years in the Steel Structures Group at that University. After some time as a consultant in steel and concrete structures he joined the Structural Engineering and Mechanics Group at the Faculty of Architecture and Building of the Eindhoven University of Technology.

J. F. G. JANSSEN

Assist. Professor
Eindhoven Univ. of Technology
Eindhoven, The Netherlands

Ir. J. F. G. Janssen, born in 1941 took his degree in architectural engineering at Delft University of Technology in 1971. Since his graduation he has combined his architect's practice with lecturing at the department of Architecture and Building Technology of the Eindhoven University, until 1986 in the Architectural Design Group, since then in the Structural Engineering Group.

SUMMARY

This paper presents a new concept in house production by industrialization of the house building process. The concept combines three essential points: Design-independent mass production; considerable influence of occupant's wishes on lay-out and finish in combination with industrialized production; optimal use of CAD-CAM in design, production and logistic management.

RÉSUMÉ

Cet article présente une nouvelle conception pour la production de maisons par industrialisation du processus de construction de l'habitat. Le concept combine les trois points essentiels suivants: Projet indépendant des moyens de production; prise en compte de l'influence des souhaits exprimés par les habitants sur l'aménagement et les finitions en combinaison avec l'industrialisation; utilisation optimale de CAD-CAM pour le projet, la production et la logistique.

ZUSAMMENFASSUNG

Dieser Beitrag beschreibt ein neues Konzept des Häuserbaues durch Industrialisierung des Bauvorganges. Das Konzept kombiniert die drei wesentlichen Punkte: entwurfsunabhängige Massenproduktion; wesentlicher Einfluss der Bewohnerwünsche bezüglich Grundrissgestaltung und Verarbeitung; optimale Verwendung von CAD-CAM in Entwurf, Produktion und Logistik.



1 INTRODUCTION

Traditional house building as well as that carried out by the mechanized building trade, has up till now, been characterized by a purely traditional organization. This is evident from the fact that in both cases

"all houses are build according to a design made in advance".

Where this concerned single homes for private persons there is nothing wrong. But when mechanized building nowadays put up for preference with one single design, the largest possible number of dwellings with the least possible variation, then there is something radically wrong. The result is then monotonous mass housing. Pressure by the community and the occupants has resulted in limiting the number of dwellings per design and per town district. Sometimes a certain variation in the site plans and finishing was brought about, but always at higher cost.

What is remarkable here is that the industrial production has at the same time been rendered powerless to participate in the house building process. This is just opposite of what would have been expected, in fact that giving preference to industrialization was the cause of suppression of the influence of the individual choice on design. But bypassing of the individual was neither the cause nor the effect of industrialization. This is clearly argued by Professor N.J.Habraken [1].

For good comprehension of what follows, we must first make a clear distinction between industrialization and prefabrication, both of which are essential to the rest of the argument. This distinction was made by Professor Habraken and for that reason a description as given in [2] will be used.

"For the past 25 years or more, a kind of confusion seems to have been plaguing discussions on innovation in housing design and production. These on technical innovation, for example, often confuse two distinct kinds of production.

When we discuss the production of houses, perhaps we can say that, when elements or parts used for building houses are made before the specific place where they will be positioned is known, (i.e. before there is a house design), we have what can be called industrialized production.

If on the other hand, when parts are made for building houses after the specific place where they will be used is known (after we have a design), then we call it prefabrication. Many things are prefabricated, on and off-site, using industrially produced parts, but only after a design has been made to guide their assembly.

Habraken made this distinction, which is held to be important to the health of a housing industry [3]. The reason the distinction is important is that the debate should be about what general parts should be industrially produced because, to be efficient, our industries need to know what to produce before house designs are made. Yet these parts need to be of a nature that they invite interpretation in diverse applications by different parties (flexibility). What general parts make sense?"

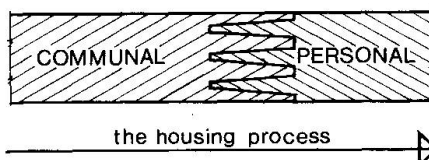
Therefore the goal of our research is an answer to this question, by:

"Design independent mass production for the housing process"

To make clear the way we tried to reach the right concept, we will follow Professor Habraken's line of thought beginning with his own statement:

"In order to solve the housing problem we must stop wanting to build dwellings".

For him a dwelling is not just something that can be designed or made; it is the result of a housing process. The last act in this process is that of the occupant who will live there.



Seen as a process the house is: . Terminus of a series of communal services.
 . . Start of a personal enterprise.

Habraken therefore sees the process of housing in two spheres:

1. the SUPPORT → for which the community is responsible and the community decides
2. the INFILL → for which the inmates make their personal decisions.

Knowledge and agreement of the two spheres makes it possible to start good application of our technical ability. In opposite, the idea of converting a completely designed dwelling into an industrially produced dwelling led to a mental blockage. It has destroyed the clear purpose of building and has rendered industrial production powerless to participate in the housing process.

In my opinion the housing industry in Japan also suffers under this mental blockage. For the five biggest Japanese producers of prefabricated dwellings, which achieved an annual production of some hundreds of thousands of prefab dwellings, mostly worked on the basis of the modular, volume-enclosing element type consequently with big, completely-designed half or third parts of houses.

According to the director of Daiwa House Industry (28.000 houses per year): [4] "There are more than 5000 different types of parts. One unit of housing requires about 600 parts based on 150 varieties, which calls for small lot production of an extremely large range of items, even in comparison with such large scale enterprises as the automobile industry.

Recently, home buyers' demands have become highly diversified, so that standardised designs no longer satisfy their requirements. This trend has been gaining even greater momentum.....

..... Currently, the gradual increase in the market share of prefabricated housing is not so much due to the lower costs brought about by mass production, (mass production is out of the question, in fact there is only small-lot production (J.O. Bats)) as was originally intended, since cost does not differ significantly from conventional housebuilding methods, but rather uniformity of quality, high performance, financial and technical credibility of the manufacturers, accessibility of advice from highly trained and experienced technical personnel and excellent after sales service".

This quotation makes it clear that to try and start a housebuilding industry based on standardized design does not work well, neither for the occupants who don't have any possibility for a personal say, nor for the industry so long as this leads to small-lot production. Which is the same as has been said above by: rendered the industrial production powerless to participate in the housing process.

The new concept presented is this contribution couples, a high degree of influence by the occupant to industrial production.

Contrary to the superficial opinion generally held, the following statement holds:

"Industrialization in the building process nowadays is the only way to reintroduce the influence of the individual.

Habraken intended the mechanized building trade to build supports, while the infill is to be produced by industry. We aim at a more complete industrialization of the housebuilding process by industrializing the support as well as the infill.

2 THE SUPPORT

Conclusions of a literature study, [5] made earlier, are that "the general parts" have to be developed with due observance of the following conditions.

- a. The design must be based on the S.A.R.⁽¹⁾ method of designing and on modular coordination.
- b. The components must be comparatively small.
- c. The components must be demountable.
- d. The components must be as "simple" as possible.
- e. The network of lines and pipes must be very much independent of the other construction components.
- f. Free choice to position the stairs must be given.

(1) S.A.R.: Stichting Architecten Research (Foundation for architectural Research)



This has resulted in a steel bearing structure of cold-formed steel-sheet, which can be considered as the basic part of a steel support for application in housebuilding [6]

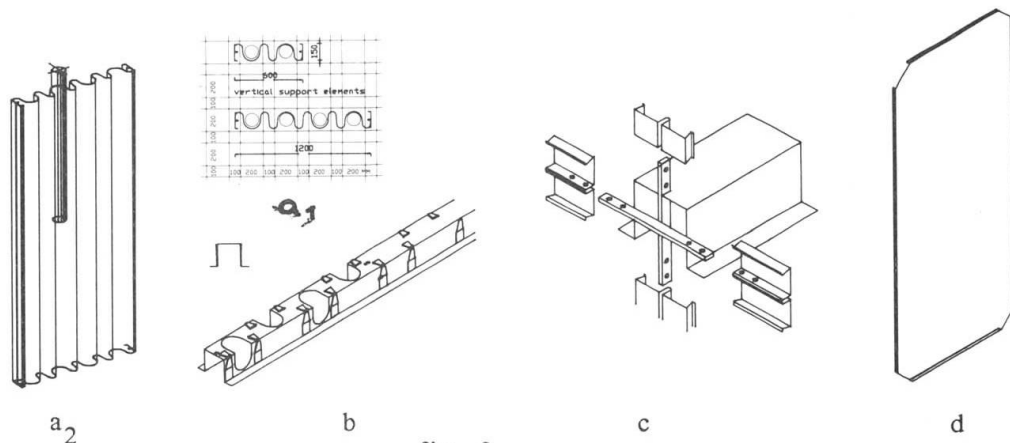


fig. 2

The core of the bearing system is the element given in figure 2a₂.

These elements are used both in the horizontal as well as in vertical direction in two widths: 600 mm and 1200 mm. (fig. 2a₁). Steel bearing elements of this kind, together with a so-called "hat profile" (fig. 2b) form the "bearing structure" of the support. The "hat profile" allows the positioning and connection of the horizontal and vertical elements of the bearing structure. Therefore, small parts are spotwelded on the outer and upper sides of the "hat". For securing the horizontal and vertical coherence, coupling strips are needed as given in fig. 2c.

The "house of cards" still requires stability provisions in the form of steel-sheet shear walls in the transversal direction. These walls are suitably placed parallel to the front and back faces of the building. (fig. 2d).

To form a support by using the steel bearing system, the permanent parts of the lines and pipes have to be installed at first followed by the subsystems for the floating floor (a), prepositioned wallpanel (b) and the ceiling (c) as shown in fig. 3 and 4.

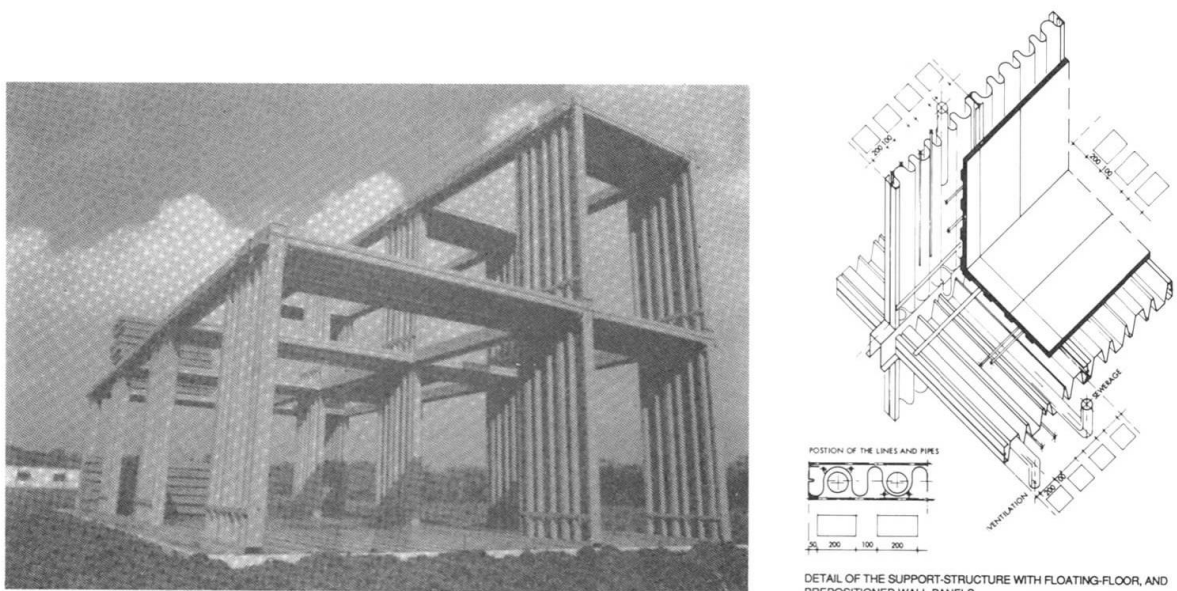


Fig. 3



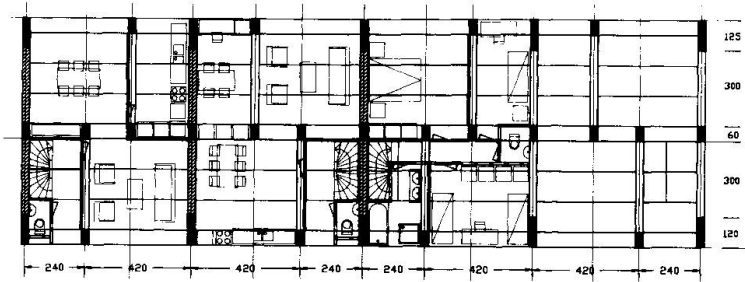
- [1] Habraken, N.John, "Three r's for housing", Scheltema en Holkema. Amsterdam 1970.
- [2] Article by Kendall and Sewada, "Changing patterns in Japanese housing", Open House Int. Vol.12, No.2, 1987.
- [3] Habraken, N.John, "Transformations of the Site, Awater Press, Cambridge, Mass. 1983.
- [4] Togo, T., "Industrialized housing in Japan: steel-frame prefabricated houses", 20 I.I.S.I. Conference, Rio de Janeiro, 5-8 October 1986.
- [5] Bats, ir. J.O. en Thijsen, ir. A.P. "Stalen Drager I", April 1983.
- [6] Bats, ir. J.O. and Janssen ir. J.F.G., "Industrialized Housing with sheet-steel elements". Ninth International Speciality Conference on Cold-Formed Steel Structures, St. Louis, Missouri, U.S.A., November 8-9, 1988.
- [7] Naoto Sasaki and Danor Hutchins, "The Japanese Approach to product quality", Pergamon press Oxford.



4 EXAMPLE

Page 5 gives an example of popular type of Dutch dwellings.

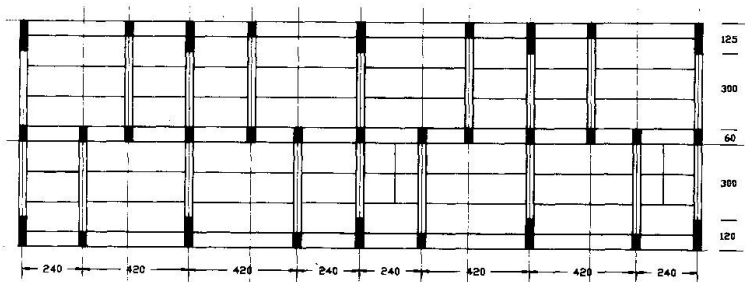
Example of different possibilities by the same support.



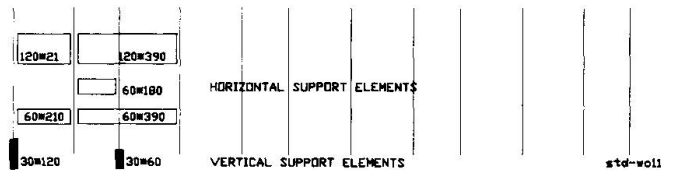
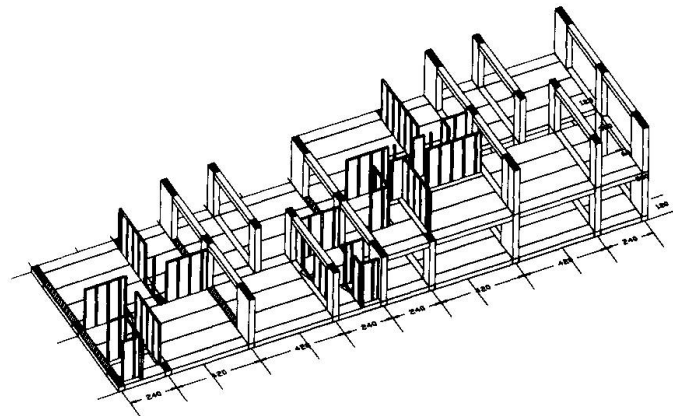
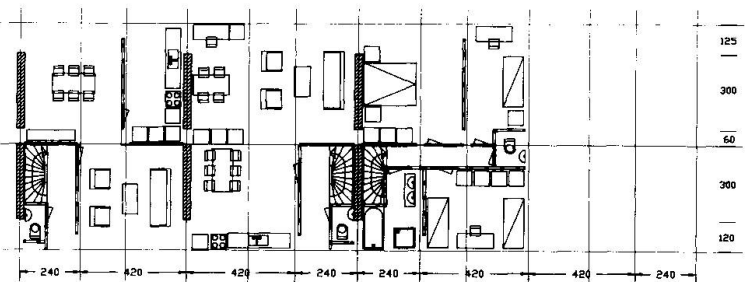
ground floor

upper floor

SUPPORT



INFILL
thereabout-occupants
makes their own
decisions.



Assessment of Fatigue Failure in Steel Arch Bridges

Estimation de la rupture de fatigue de ponts en arc métalliques
Beurteilung des Ermüdungs-Versagens einer Stahl-Bogenbrücke

Shigeyuki MATSUI
Associate Professor
Osaka University
Osaka, Japan



Jinichiro SAKAI
Civil Engineer
Hitachizosen Co.
Osaka, Japan



Ahmed S. EL-HAKIM
Graduate Student
Osaka University
Osaka, Japan



Shigeyuki Matsui, born in 1943 earned his D. Eng. at Osaka University. He works at Osaka University since 1971. He is now interested in deterioration and fatigue of highway bridges.

Jinnichiro Sakai, born in 1946, earned his M. Eng. at Kyoto University. He works at Hitachizosen Co. since 1973. He is now interested in fatigue design method of highway bridges.

Ahmed El-Hakim, born in 1953, earned his M. Eng. at Al-Azhar University. He is studying to get the Doctor of Eng. degree at Osaka University.

SUMMARY

On deck-type arch bridges, severe fatigue cracks have been found at joints of the strut and arch rib. These cracks have been assessed through fatigue analysis using simulated natural vehicle rows by computer. The main external cause of these cracks was due to the alternating stresses at the joint which is generated by traffic. Traffic management is finally discussed with reference to the parameter analysis for fatigue life.

RÉSUMÉ

Sur les ponts en arc à tablier supérieur, d'importantes fissures ont été découvertes au niveau des raccords de nervure de cintre et d'entretoise. Ces fissures ont été évaluées grâce à des analyses de fatigue par ordinateur en observant le trafic routier. La cause extérieure principale de ces fissures est liée aux efforts alternés au droit des joints dus aux passages des véhicules. Le contrôle du trafic a été déterminé en fonction des données paramétriques concernant le cycle de fatigue.

ZUSAMMENFASSUNG

An Bogenbrücken wurden Risse kritischer Länge im Anschlussbereich von Bogenträger und Stäben gefunden. Die Rissbildung wurde rechnergestützt simuliert; als Lastkollektive wurden repräsentative, wandernde Verkehrslasten angenommen. Als Hauptursache der Rissbildung an den Anschlüssen, konnten die durch das Lastkollektiv erzeugten dynamischen Wechsellasten bestätigt werden. Zum Schluss der Untersuchung der Lebensdauer-Parameter wird der Einfluss verkehrsregelnder Massnahmen erörtert.



1. INTRODUCTION

In Japan, many deck type arch bridges have been built from the point of view of aesthetics and structural reliability. However, fatigue cracks have been frequently observed at the joints of struts with arch ribs in the bridges built until about ten years ago.

The struts have been designed as a column members loaded by reaction forces from floor systems, which were calculated using a simplified triangle influence lines. However, the actual struts are subjected to in-plane and out-of-plane bending moments due to deformation of the arch rib and fixation at joints. Furthermore, the joints of the struts with arch rib are subjected to alternating stresses by running vehicles on the bridge. Therefore, although poor consideration for details of the welding joints seems to be one reason for the cracks, missing of three-dimensional structural behavior at the original design and of the effect of vehicle loading seem to be main causes.

In this paper, fatigue assessments for a typical arch bridge were carried out by the latter two causes. That is, the effects of three dimensional behavior and of traffic loadings characteristics were evaluated through a simulation analysis of traffic flows and vehicle loads. Then, some traffic management methods in order to extend the remaining fatigue life of same type of arch bridges were discussed.

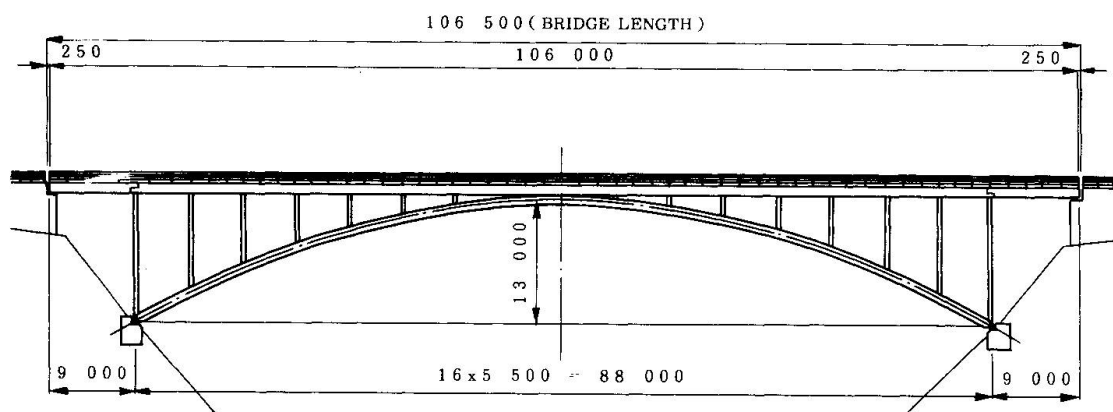


Fig. 1 General View of Deck Arch Bridge

2. BRIDGE MODEL AND S-N RELATION FOR THE ASSESSMENT

Fig.1 shows the arch bridge to be assessed. It was designed by the allowable stress design method and was built in 1963. The details of the jointing between a strut and the arch rib are shown in Fig.2. The gusset plates were welded to arch rib by fillet welding which forms a cruciform welding joint. The joints of No. - were really damaged by fatigue cracks after only 12 years service.

The laboratory fatigue data for the cruciform welding joint as shown in Fig.3 can be applied for the assessment. The equation for the median S-N curve shown in Fig.3 was obtained by a linear regression analysis. The curve seems to be suitable for the assessment because fatigue cracks have occurred at many points.

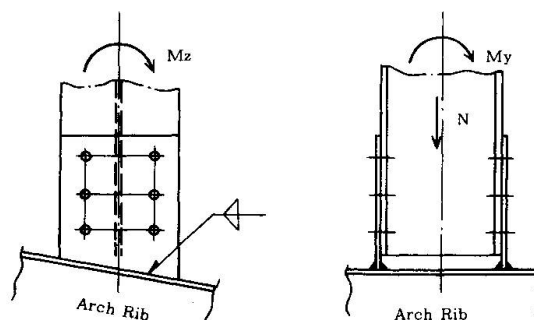


Fig. 2 Detail A

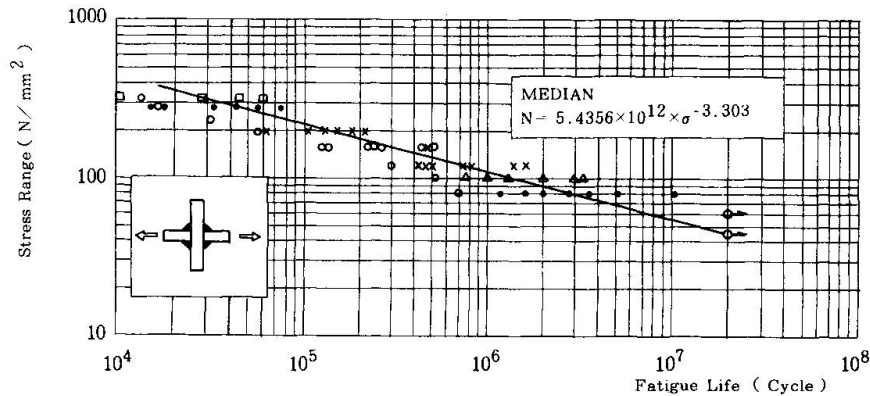


Fig. 3 Fatigue Properties for Load-Carrying Cruciform Welded Joints

3. METHOD OF ASSESSMENT

3.1 FATIGUE DAMAGE RULE

The effect of variable stress amplitude on fatigue is accounted with the cumulative damage rule called as Palmgren-Miner hypothesis. Failure occurs when the damage rate under variable stress amplitude (S_i) satisfies Eq.(1).

$$D = \sum D_i = \sum (n_i \cdot Y_f / N_i) \geq 1 \quad (1)$$

where, n_i : repetition cycles in one year by an arbitrary stress range S_i ,

$$Y_f \cdot N_{eq} = Y_f \sum n_i (S_i / S_{rd})^m \geq N_f \quad (2)$$

$f(s)$: stress probability function,

N_0 : traffic volume in one year,

Y_f : fatigue life in year,

N_i : fatigue life at the stress range S_i .

On the other hand, when the equivalent repeating cycles by computing Eq.(2) becomes equal to the fatigue life by the fixed standard stress S_{rd} , fatigue cracks will occur.

$$n_i = N_0 \int_{S_i}^{S_{i+1}} f(x) dx \quad (3)$$

where, S_i : arbitrary stress range due to random loading,

S_{rd} : a standard stress range,

m : inverse of absolute of the slope of S-N curve,

At the actual bridge, the traffic volume of large trucks has been reported as about 1000/day. Using this number, the total daily traffic volume can be calculated by the composition of vehicles. Then, probability density function of stress range were obtained by doing simulation analysis for the traffic volume of one year. After that, N_{eq} for one year based on a standard stress level S_{rd} can be obtained and the fatigue life N_f at the stress range S_{rd} . Finally, the fatigue life represented by years can be obtained by Eq.(4).

$$Y_f = N_f / N_{eq} \quad (4)$$

3.2 SIMULATION ANALYSIS FOR STRESS RANGE DISTRIBUTION

As mentioned above, the fatigue cracks seem to be due to repetition of large bending stresses at the joint. Since those bending stresses will occur at random due to natural traffic flow, the probability density function has to be obtained through simulation analysis. Two-dimensional frame analysis is common in the



recent design. However, actual structures behave in three-dimensions. So, the assessments were carried out with the stress results of the both two- and three-dimensional analyses.

Fig.4 shows the flow of simulation analysis. The outline of the analysis can be explained as follows:

(1) Firstly, the influence lines have to be created for the aimed points. The root of welding of the damaged joints were focused. Here, the influence lines of in-plane and out-of-plane bending moment and axial force regarding to the roots were prepared by the two- and three-dimensional analyses.

(2) Using the probability characteristics of vehicle weight and composition ratio of vehicles, the rows of vehicle weight are generated with Monte Carlo simulation method.

(3) The row of weight is rearranged by the natural traffic flow characteristics such as gaps of vehicles, passing position and dimensions of vehicles. The probability density functions of the gaps and the passing position are Log-Normal distribution of $LN(200m, 58.1m)$ and Normal distribution of $N(1.303m, 0.24m)$, respectively. The impact ratio is supposed by $N(0.044, 0.055)$.

(4) All vehicle weights are divided into axle loads because the stresses at the aimed point seem to be due to local loading of axles.

(5) The arranged axle weights are moved on the influence line on the bridge. Every one meter movement, the total stresses at the aimed point is calculated. Then, the stress series in real time are obtained.

(6) Stress range distribution is obtained from the series by the rain flow method. Finally, equivalent number of cycles N_{eq} can be estimated by Eqs.(2) and (3).

3.3 INPUT DATA

The Ministry of Construction and Hanshin Expressway Public Corporation etc. have published their traffic data obtained from field measurements. The authors have also carried out several field measurements to establish the characteristic of traffic loads on national highways. Those data shown in Table 1 were used for the assessments. Data (A) seems to represent the traffic characteristics on national highway, Data (B) represents the one on urban elevated highway and the Data (C) represents typical traffic characteristics in a commercial city.

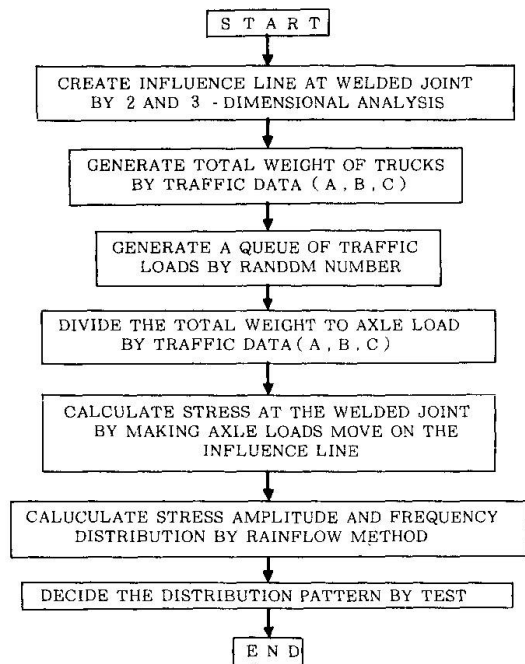


Fig. 4 Flow Chart of Fatigue Analysis

	No	Vehicles	Distri. Pattern	Weight (N)		
				Max	μ	σ
A	①	Car	LN	30.4	12.7	3.5
	②	S.T	LN	123.5	35.3	13.2
	③	M.T	LN	179.3	63.7	24.5
	④	L.T1-2	LN	443.0	166.6	61.7
	⑤	L.D1-2	LN	606.6	196.0	96.0
	⑥	L.T2-1	LN	330.3	156.8	68.6
	⑦	TRL	LN	849.7	294.0	117.6
	⑧	BUS	LN	183.3	135.2	23.5
B	①	Car	LN	28.4	13.4	3.6
	②	M.T	LN	126.4	48.7	29.3
	③	L.T2 (NL)	N	359.7	74.9	20.9
	④	" (L)	LN	359.7	139.0	25.6
	⑤	" (OL)	EXP	359.7	217.6	21.6
	⑥	L.T1-2 (NL)	N	370.4	112.8	20.7
	⑦	" (L)	LN	370.4	203.8	33.0
	⑧	" (OL)	EXP	370.4	316.4	22.4
	⑨	TRL (NL)	N	670.3	134.0	20.3
	⑩	" (L)	LN	670.3	250.9	104.6
C	①	Car	LN	19.6	13.13	2.84
	②	S.T	LN	124.5	31.07	15.88
	③	L.T 2	LN	176.4	60.47	37.73
	④	L.T2-1	LN	205.8	162.68	62.33
	⑤	L.T1-2	LN	284.2	136.81	37.83
	⑥	TRL	LN	460.6	235.59	115.35

S.T : Small Truck
M.T : Medium Truck (2 - axes)
L.T1 - 2 : Large Truck (Rear Tandem)
L.D1 - 2 : Large Dump (Rear Tandem)
L.T2 - 1 : Tank Rolly (Front Tandem)
L.T2 : Large Truck (2 - axes)
TRL : Trailer

Table 1 Constitution of Traffic (Data (A)/(B)/(C))

4. ASSESSMENT RESULTS FOR FATIGUE LIFE

Fig. 5 is the obtained frequency distributions of stress amplitude at the aimed point due to three traffic data. These distributions can be fit by a Weibull distribution function. Fig.6 shows the comparison of fatigue damage D_i of every stress level at fatigue failure by the three traffic data. The difference of the traffic characteristics became clear by this figure.

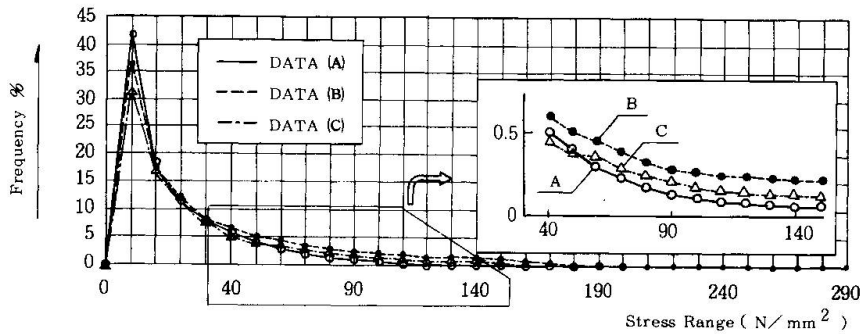


Fig. 5 Frequency Distribution of Stress Range

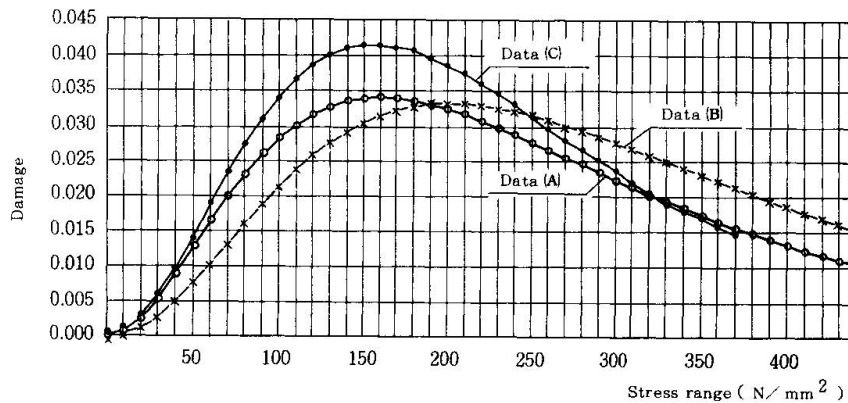


Fig. 6 Failure Probability (Data (A) , Data (B) , and Data (C))

The results of Y_f for three traffic data are shown in Figs. 7. The actual fatigue life was about 12 years. For the life, the results of Data(A) and Data(C) firstly seem to be right because the actual bridge is located in a national highway and can be supposed to be subjected to similar traffic load characteristics of those Data. Secondly, the difference of assessed fatigue lives by two- and three-dimensional analysis has to be paid attention. Three-dimensional analysis gives significantly shorter life than two-dimensional one. The difference is attributed to out-of-plane bending moment acting on struts. Actually, as the joints are subjected to three-dimensional stresses, the result of three-dimensional analysis should be considered more rigorous. Therefore, the result of three-dimensional analysis of Data(A) can be concluded as the rigorously assessed life.

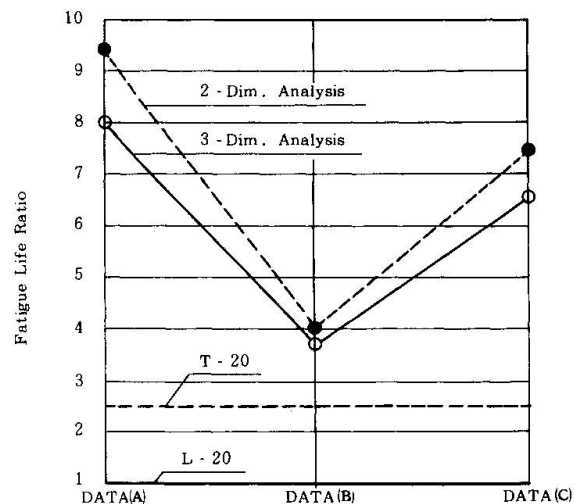


Fig. 7 Comparison of Fatigue Life in Each Data



5. DISCUSSION FOR EXTENSION OF FATIGUE LIFE

Now, as there are many same type of arch bridges, the safety for fatigue of those bridges have to be checked. If any fatigue damage does not occur yet, we have to do some effort to extend the remaining fatigue life. Three kinds of method can be considered. The first is reinforcement for the connection parts which actually carried out for the bridge. The second is to do regulation to prohibit simultaneous loadings of heavy trucks, and the third is a regulation of the maximum weight of trucks.

5.1 Regulation for simultaneous loading of truck

To make clear the influence of simultaneous loading of vehicles on the bridge, the simulation by single vehicle loading was done using the same traffic condition of Data(A). The fatigue life increased to about 47.8 times of common traffic flow under which simultaneous loading were allowed. From the results, traffic regulation seem to be an effective method to extend of the fatigue life. The regulation can be done by setting prohibition traffic signs on the both entrance of the bridge.

5.2 Regulation of truck weight

Fig.8 is the results of the simulation analyses using Data(A) by limiting the maximum vehicle weight up to the values shown in the Figure. As the result, the limitation of the maximum weight of large truck also can be recognized to be very effective. In Japan, the design service life of 50 years is very common. If the fatigue life Y_f is shorter than 50 years, the remaining life $Y_r = (Y_f - Y_i)$, here Y_i is the service period from the construction to the inspecting time in year, should be extend to $Y_r = (50 - Y_i)$ according to the maximum vehicle loads by using the ratio of the fatigue life which can be calculate from the curve of Fig.8. The limitation seem to be possible with a traffic signs and some enforcement by policemen.

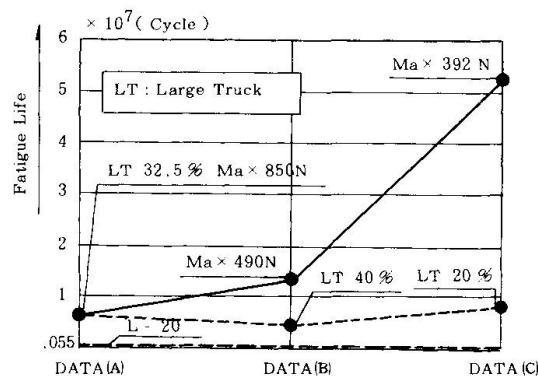


Fig. 8 Influence to Fatigue Life due to Max Truck Weight and Occurrence Ratio of Large Truck

6. CONCLUSIONS

The fatigue life of an existing arch bridge was discussed. The simulation analysis using actual traffic data can make possible for such an assessment. The main conclusions are :

- (1) The fatigue life of actual arch bridge can be correctly assessed under actual traffic loadings generated by simulation analysis.
- (2) The main cause of the fatigue cracking seems to be due to the simultaneous loading of heavy trucks which was not considered in the original design.
- (3) For the extension of fatigue life of existing same type of arch bridges, regulation of the maximum truck weight is the most effective method.

7. REFERENCES

- 1) The Minist. of Const.: A Study of Design Live Load on LSD Method, 1989,1.
- 2) Hanshin Expressway Public Corpo.: Rept. of Committee on Design Load, 1984,3.
- 3) Japan Road Associ.: Specification for Highway Bridges Part 2, 1980,2.
- 4) J.W.Fisher: Fatigue and Fracture in Steel Bridges, John Willey & Sons.